J Bone Miner Metab (2005) 23:226–230
DOI 10.1007/s00774-004-0588-x

ORIGINAL ARTICLE

**Tomohiko Urano · Masataka Shiraki · Masayo Fujita
Takayuki Hosoi · Hajime Orimo · Yasuyoshi Ouchi
Satoshi Inoue**

Association of a single nucleotide polymorphism in the lipoxygenase *ALOX15* 5′-flanking region (−5229G/A) with bone mineral density

Received: October 22, 2004 / Accepted: November 16, 2004

Abstract The 12/15-lipoxygenase gene *Alox15* has been identified as a susceptibility gene for bone mineral density (BMD) in mice through combined genetic and genomic analyses. Here we studied the association between bone mineral density and an *ALOX15* gene single nucleotide polymorphism to assess the potential involvement of the human *ALOX15* gene in postmenopausal osteoporosis. Specifically, we examined the association between a single nucleotide polymorphism at −5299G/A in the *ALOX15* 5′-flanking region with BMD in 319 postmenopausal Japanese women (66.7 ± 8.9 years, mean ± SD). We found that subjects bearing at least one variant A allele (GA + AA; $n = 273$) had significantly lower Z scores for lumbar spine and total body bone mineral density than did subjects with no A allele (GG; $n = 46$) (lumbar spine, −0.25 ± 1.34 versus 0.48 ± 1.70; $P = 0.0014$; total body, 0.25 ± 1.01 vs 0.62 ± 1.11; $P = 0.048$). These findings suggest that the *ALOX15* gene is one of the genetic determinants of BMD in postmenopausal women. Accordingly, this polymorphism could be useful as a genetic marker for predicting the risk of osteoporosis.

Key words Adipogenesis · *ALOX15* · PPARγ · Osteoporosis · Bone mineral density · Polymorphism

T. Urano · M. Fujita · Y. Ouch · S. Inoue (✉)
Department of Geriatric Medicine, Graduate School of Medicine, University of Tokyo, 7-3-1 Hongo, Bunkyo-ku, Tokyo 113-8655, Japan
Tel. +81-3-3815-5411; Fax +81-3-5800-6530
e-mail: INOUE-GER@h.u-tokyo.ac.jp

M. Shiraki
Research Institute and Practice for Involutional Diseases, Nagano, Japan

M. Fujita · S. Inoue
Research Center for Genomic Medicine, Saitama Medical School, Saitama, Japan

T. Hosoi
Tokyo Metropolitan Geriatric Hospital, Tokyo, Japan

H. Orimo
Health Science University, Yamanashi, Japan

Introduction

Osteoporosis is characterized by low bone mineral density (BMD), increased bone fragility, and consequently increased risk of fracture [1]. Studies of twins and siblings have shown that BMD is under genetic control, with estimates of heritability ranging from 50% to 90% [2,3]. BMD is regulated by interaction of multiple environmental and genetic factors, each having modest effects on bone mass and bone turnover [4,5]. Polymorphisms of several genes have been investigated to clarify the determinants of BMD [6,7]. These genes of which polymorphisms were associated with BMD include those implicated in bone formation by regulation of osteoblast growth and function, such as *vitamin D receptor* gene [8], *transforming growth factor beta-1* (*TGFβ1*) gene, *collagen type Iα1* (*COLIA1*) gene [9], *peroxisome proliferator-activated receptor-γ* (*PPARγ*) gene [10], and *low-density lipoprotein receptor-related protein 5* (*LRP5*) gene [11]. Identification of candidate genes that affect bone mass will be useful for early detection of individuals who are at risk of osteoporosis for early institution of preventive measures.

The decrease in bone volume associated with osteoporosis is accompanied by an increase in marrow adipose tissues [12,13]. Indeed, an increase in marrow adipocytes is observed in several conditions that lead to bone loss, such as ovariectomy [14], immobilization [15], and treatment with glucocorticoids [16]. Recent studies have identified rodent quantitative trait locus associated with increased BMD in the mouse gene encoding 12/15-lipoxygenase [17], the enzyme that converts linoleic acid and arachidonic acid into endogenous ligands for the PPARγ [18–20]. Activation of this pathway in marrow-derived mesenchymal progenitors stimulates adipogenesis and inhibits osteoblastogenesis [21,22]. Mice that are deficient in this gene or have been treated with 12/15-lipoxygenase inhibitors demonstrate increased bone mass as compared with controls [17]. These findings suggest that genetic variants of the 12/15-lipoxygenase encoding gene may affect the BMD in humans as well as mice. The mouse 12/15-lipoxygenase enzyme

corresponds to at least three lipoxygenases in humans. 15-Lipoxygenase has two isoenzymes: type 1 (human *ALOX15*, encoded by a gene at chromosome 17p13.3) and type 2 (human *ALOX15B*, encoded by a separate gene at 17p13.1). 12-Lipoxygenase (human *ALOX12*, encoded by a gene at chromosome 17p13.1) is predominantly expressed in platelets and macrophages and is distinct from 15-lipoxygenase [23]. In the present study, we examined the possibility that there is an association between a polymorphism in the human *ALOX15* gene and BMD in Japanese women to investigate the possible contribution of the lipoxygenase to bone metabolism.

Subjects and methods

Subjects

We analyzed genotypes in DNA samples from 319 healthy postmenopausal Japanese women (66.7 ± 8.9 years, mean ± SD). We excluded women having endocrine disorders such as hyperthyroidism, hyperparathyroidism, diabetes mellitus, liver disease, and renal disease; those who used medications known to affect bone metabolism (e.g., corticosteroids, anticonvulsants, and heparin); and those with an unusual gynecological history. All subjects were unrelated volunteers. Each subject provided informed consent before entering the study.

Measurement of bone mineral density and biochemical markers

We measured the lumbar spine BMD and total body BMD of participants by dual-energy X-ray absorptiometry using the fast-scan mode (DPX-L; Lunar, Madison, WI, USA). The BMD data were recorded as *Z* scores, as the deviation from the weight-adjusted average BMD for each year of age, based on data from 20000 Japanese women. We also measured each subject's serum concentrations of alkaline phosphatase (ALP), intact osteocalcin (I-OC), intact parathyroid hormone (PTH), calcitonin, 1,25-$(OH)_2D_3$, total cholesterol (TC), and triglyceride (TG). We also measured urinary ratios of deoxypyridinoline (DPD) to creatinine using the high pressure liquid chromatography (HPLC) method.

Determination of a single nucleotide polymorphism in the ALOX15 gene

We extracted a polymorphic variation of the putative *ALOX15* gene promoter/enhancer region from the Assays-on-Deman SNP Genotyping Products database (Applied Biosystems, Foster City, CA, USA) and, according to its localization on the gene, denoted it −5299 G>A. We determined the −5299G/A polymorphism of the *ALOX15* gene using the TaqMan (Applied Biosystems) polymerase chain reaction (PCR) method [24]. To determine the *ALOX15* SNP we used Assays-on-Demand SNP Genotyping Products C_926671_10 (Applied BioSystems), which contains sequence-specific forward and reverse primers and two TaqMan MGB probes for detecting alleles. During the PCR cycle, two TaqMan probes competitively hybridize to a specific sequence of the target DNA and the reporter dye is separated from the quencher dye, resulting in an increase in fluorescence of the reporter dye. The fluorescence levels of the PCR products were measured with the ABI PRISM 7000 (Applied Biosystems), resulting in clear identification of three genotypes of the single nucleotide polymorphism (SNP).

Statistical analysis

We divided subjects into those having one or two chromosomes of the major A allele and those with only the minor G allele encoded at the same locus. Comparisons of *Z* scores and biochemical markers between these two groups were subjected to statistical analysis (Student's *t* test; StatView-J 4.5). A *P* value of less than 0.05 was considered statistically significant.

Results

Association of ALOX15 gene polymorphism with bone mineral density

Among our 319 subjects, 46 were GG homozygotes, 155 were GA heterozygotes, and 118 were AA homozygotes. Allelic frequencies were 0.613 for the A allele and 0.387 for the G allele in this population. The allelic frequencies of this SNP in the present study were in Hardy–Weinberg equilibrium.

We compared the 273 subjects bearing at least one chromosome with the A allele (genotype GA + AA) and the 46 subjects having no A allele (GG) with respect to their *Z* scores for lumbar spine and total body BMD. Those with the A allele had significantly lower *Z* scores for lumbar spine BMD (−0.25 ± 1.34 vs 0.48 ± 1.70; $P = 0.0014$) (Fig. 1A) and total body BMD (0.25 ± 1.01 vs 0.62 ± 1.11; $P = 0.048$) (Fig. 1B). As shown in Table 1, the background and biochemical data did not significantly differ between these groups.

Discussion

Various regulating elements have been identified within the *ALOX15* 5′-flanking promoter/enhancer region, including a site for binding with Sp1 [25], AP1 [25], and GATA [26], as well as sites for methylation [27] and acetylation [28,29] and a Stat6 response element [29], suggesting that 15-lipoxygenase expression is directly regulated through transcription regulation. In the present study, we observed a significant association between BMD and a G/A SNP at the

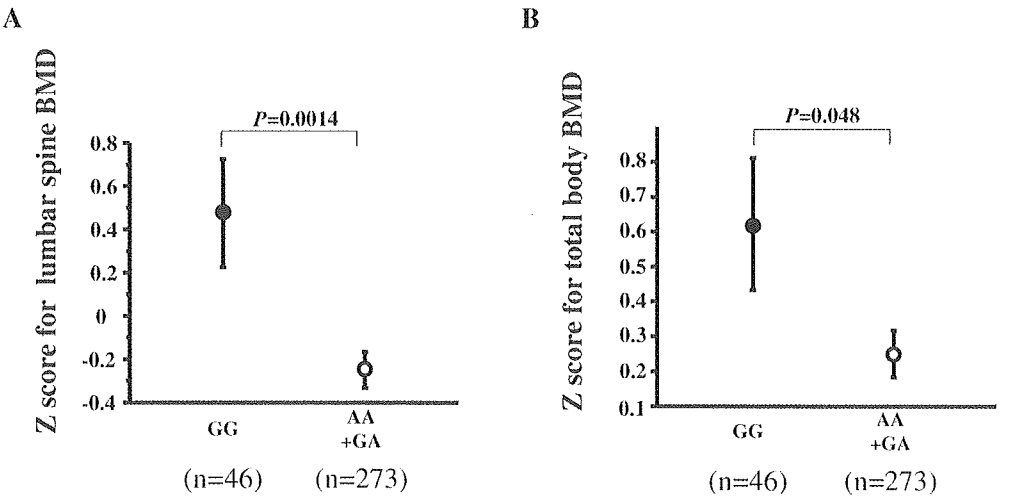

Fig. 1. *Z* scores of lumbar spine and total body bone mineral density (BMD) in subject groups with each genotype of *ALOX15* gene polymorphism in the 5′-flanking region (−5229G/A). **A** *Z* scores for lumbar spine BMD are shown for genotype AA + GA and genotype GG. Values are expressed as mean ± SE. Numbers of subjects are shown in *parentheses*. **B** *Z* scores for total body BMD are shown in the same manner as in **A**

Table 1. Comparison of background, BMD and biochemical data between subjects bearing at least one A allele (AA + GA) and subjects with no A allele (GG) in the *ALOX15* gene 5′-flanking region (−5299G/A)

Items	Genotype (mean ± SD)		*P* value[a]
	GG	GA + AA	
Number of subjects	46	273	
Age (years)	69.0 ± 8.9	66.3 ± 8.9	NS
Height (cm)	149.5 ± 6.9	150.3 ± 6.1	NS
Body weight (kg)	49.6 ± 8.6	50.3 ± 7.9	NS
Lumber spine BMD (*Z* score)	0.48 ± 1.70	−0.25 ± 1.37	0.0014
Total body BMD (*Z* score)	0.62 ± 1.12	0.25 ± 1.01	0.048
ALP (IU/l)	185.6 ± 63.9	193.4 ± 66.0	NS
I-OC (ng/ml)	8.2 ± 3.2	7.8 ± 3.6	NS
DPD (pmol/μmol Cr)	7.0 ± 3.0	7.6 ± 2.7	NS
Intact PTH (pg/ml)	38.6 ± 20.0	35.2 ± 15.1	NS
Calcitonin (pg/ml)	16.6 ± 4.5	23.1 ± 11.4	NS
1,25-$(OH)_2D_3$ (pg/ml)	33.0 ± 7.7	35.7 ± 11.8	NS
TC (mg/dl)	193.0 ± 45.0	199.4 ± 36.5	NS
TG (mg/dl)	142.5 ± 74.0	142.4 ± 81.8	NS
% Fat	32.1 ± 6.6	31.9 ± 7.7	NS
BMI	22.1 ± 3.0	22.1 ± 3.1	NS

BMD, bone mineral density; ALP, alkaline phosphatase; I-OC, intact-osteocalcin; DPD, deoxypyridinoline; Cr, creatinine; PTH, parathyroid hormone; TC, total cholesterol; TG, triglyceride; BMI, body mass index; NS, not significant

[a]Statistical analysis was performed according to the method described in the text

−5299 site in the *ALOX15* 5′-flanking region. This is the first report to our knowledge that a common SNP in the *ALOX15* gene affects BMD. One possible explanation for this effect is that this 5′-flanking region polymorphism may be involved in the newly defined transcriptional regulating element of the *ALOX15* promoter/enhancer. Alternatively, the 5′-flanking region polymorphism may have a linkage with another base of the *ALOX15* promoter/enhancer that may control transcription of the *ALOX15* gene. It is also possible that this SNP may be linked with mutation of the *ALOX15* exons or another unidentified gene adjacent to the *ALOX15* locus, which affect the bone mass.

Although there are three lipoxygenases in humans, *ALOX15*, *ALOX15B*, and *ALOX12*, that correspond to 12/15-lipoxygenase in mice [23], we know little of their roles in human bone metabolism. Our results suggest that the 15-lipoxygenase type 1, the *ALOX15*, may have a specific function in the regulation of bone mass in human. It should be required to determine how signals from 15-lipoxygenase can be transduced to the regulation of the bone metabolism.

Three major cellular events are involved in senile osteoporosis: declining levels of osteogenesis, increasing numbers of apoptotic osteoblasts and osteocytes, and increasing levels of bone marrow adipogenesis [30–32]. The bone marrow adipogenesis that occurs with aging may be due to alterations in cell differentiation, in part by PPARγ activation [33–35] and increasing lipid oxidation [36]. Previous

reports demonstrated that 12/15-lipoxygenases are involved in this system [17,18,37,38], suggesting that 12/15-lipoxygenase may increase with aging in progenitor cells and activate adipogenesis. It has been also shown that 12/15-lipoxygenase is increased in Alzheimer's disease, which is the most common neurodegenerative disorder of the elderly [39]. Therefore, it is tempting to speculate that 12/15-lipoxygenase is increased associated with aging and senile osteoporosis. To test this hypothesis, measurement of 12/15-lipoxygenase activity and association study between BMD and the *ALOX15* gene SNP in older subjects is desirable.

In conclusion, our finding suggests that the *ALOX15* gene may be a genetic determinant of BMD in postmenopausal women. Examining the variation in the *ALOX15* gene will hopefully enable us to elucidate one of the mechanisms of involutional osteoporosis. Furthermore, the variation may be a potential genetic susceptibility factor that need to be further evaluated with regard to the risk of other diseases in which 15-lipoxygenase have been clearly implicated, including atherosclerosis [40], asthma [41], cancer [42], and glomerulonephritis [43].

Acknowledgments This work was partly supported by grants from the Japanese Ministry of Health, Labor and Welfare and the Japanese Ministry of Education, Culture, Sports, Science and Technology. We thank Ms. E. Sekine, C. Onodera, and M. Kumasaka for expert technical assistance.

References

1. Kanis JA, Melton LJ III, Christiansen C, Johnston CC, Khaltaev N (1994) The diagnosis of osteoporosis. J Bone Miner Res 9:1137–1141
2. Flicker L, Hopper JL, Rodgers L, Kaymakci B, Green RM, Wark JD (1995) Bone density determinants in elderly women: a twin study. J Bone Miner Res 10:1607–1613
3. Young D, Hopper JL, Nowson CA, Green RM, Sherwin AJ, Kaymakci B, Smid M, Guest CS, Larkins RG, Wark JD (1995) Determinants of bone mass in 10 to 26 year old females: a twin study. J Bone Miner Res 10:558–567
4. Krall EA, Dawson-Hughes B (1993) Heritable and life-style determinants of bone mineral density. J Bone Miner Res 8:1–9
5. Gueguen R, Jouanny P, Guillemin F, Kuntz C, Pourel J, Siest G (1995) Segregation analysis and variance components analysis of bone mineral density in healthy families. J Bone Miner Res 10: 2017–2022
6. Nelson DA, Kleerekoper M (1997) The search for the osteoporosis gene. J Clin Endocrinol Metab 82:989–990
7. Liu YZ, Liu YJ, Recker RR, Deng HW (2002) Molecular studies of identification of genes for osteoporosis: the 2002 update. J Endocrinol 177:147–196
8. Morrison NA, Qi JC, Tokita A, Kelly PJ, Crofts L, Nguyen TV, Sambrook PN, Eisman JA (1994) Prediction of bone density from vitamin D receptor alleles. Nature (Lond) 367:284–287
9. Uitterlinden AG, Burger H, Huang Q, Yue F, McGuigan FE, Grant SF, Hofman A, van Leeuwen JP, Pols HA, Ralston SH (1998) Relation of alleles of the collagen type Ialpha1 gene to bone density and the risk of osteoporotic fractures in postmenopausal women. N Engl J Med 338:1016–1021
10. Ogawa S, Urano T, Hosoi T, Miyao M, Hoshino S, Fujita M, Shiraki M, Orimo H, Ouchi Y, Inoue S (1999) Association of bone mineral density with a polymorphism of the peroxisome proliferator-activated receptor gamma gene: PPARgamma expression in osteoblasts. Biochem Biophys Res Commun 260:122–126
11. Urano T, Shiraki M, Ezura Y, Fujita M, Sekine E, Hoshino S, Hosoi T, Orimo H, Emi M, Ouchi Y, Inoue S (2004) Association of a single-nucleotide polymorphism in low-density lipoprotein receptor-related protein 5 gene with bone mineral density. J Bone Miner Metab 22:341–345
12. Meunier P, Aaron J, Edouard C, Vignon G (1971) Osteoporosis and the replacement of cell populations of the marrow by adipose tissue. A quantitative study of 84 iliac bone biopsies. Clin Orthop 80:147–154
13. Burkhardt R, Kettner G, Bohm W, Schmidmeier M, Schlag R, Frisch B, Mallmann B, Eisenmenger W, Gilg T (1987) Changes in trabecular bone, hematopoiesis and bone marrow vessels in aplastic anemia, primary osteoporosis, and old age: a comparative histomorphometric study. Bone (NY) 8:157–164
14. Wronski TJ, Walsh CC, Ignaszewski LA (1986) Histologic evidence for osteopenia and increased bone turnover in ovariectomized rats. Bone (NY) 7:119–123
15. Miniare P, Meunier PJ, Edouard C, Bernard J, Courpron J, Bourret J (1974) Quantitative histological data on disuse osteoporosis. Calcif Tissue Res 17:57–73
16. Wang GW, Sweet D, Reger S, Thompson R (1977) Fat cell changes as a mechanism of avascular necrosis in the femoral head in cortisone-treated rabbits. J Bone Joint Surg 59A:729–735
17. Klein RF, Allard J, Avnur Z, Nikolcheva T, Rotstein D, Carlos AS, Shea M, Waters RV, Belknap JK, Peltz G, Orwoll ES (2004) Regulation of bone mass in mice by the lipoxygenase gene Alox15. Science 303:229–232
18. Huang JT, Welch JS, Ricote M, Binder CJ, Willson TM, Kelly C, Witztum JL, Funk CD, Conrad D, Glass CK (1999) Interleukin-4-dependent production of PPAR-gamma ligands in macrophages by 12/15-lipoxygenase. Nature (Lond) 400:378–382
19. Kuhn H, Walther M, Kuban RJ, Wiesner R, Rathmann J, Kuhn H (2002) Prostaglandins Other Lipid Mediat 68–69:263–290
20. Nosjean O, Boutin JA (2002) Natural ligands of PPARgamma: are prostaglandin J(2) derivatives really playing the part? Cell Signal 14:573–583
21. Lecka-Czernik B, Moerman EJ, Grant DF, Lehmann JM, Manolagas SC, Jilka RL (2002) Divergent effects of selective peroxisome proliferator-activated receptor-gamma 2 ligands on adipocyte versus osteoblast differentiation. Endocrinology 143: 2376–2384
22. Khan E, Abu-Amer Y (2003) Activation of peroxisome proliferator-activated receptor-gamma inhibits differentiation of preosteoblasts. J Lab Clin Med 142:29–34
23. Krieg P, Marks F, Furstenberger G (2001) A gene cluster encoding human epidermis-type lipoxygenases at chromosome 17p13.1: cloning, physical mapping, and expression. Genomics 73:323–330
24. Asai T, Ohkubo T, Katsuya T, Higaki J, Fu Y, Fukuda M, Hozawa A, Matsubara M, Kitaoka H, Tsuji I, Araki T, Satoh H, Hisamichi S, Imai Y, Ogihara T (2001) Endothelin-1 gene variant associates with blood pressure in obese Japanese subjects: the Ohasama Study. Hypertension 38:1321–1324
25. Kelavkar U, Wang S, Montero A, Murtagh J, Shah K, Badr K (1998) Human 15-lipoxygenase gene promoter: analysis and identification of DNA binding sites for IL-13-induced regulatory factors in monocytes. Mol Biol Rep 25:173–182
26. Kamitani H, Kameda H, Kelavkar UP, Eling T (2000) A GATA binding site is involved in the regulation of 15-lipoxygenase-1 expression in human colorectal carcinoma cell line, caco-2. FEBS Lett 467:341–734
27. Liu C, Xu D, Sjoberg J, Forsell P, Bjorkholm M, Claesson HE (2004) Transcriptional regulation of 15-lipoxygenase expression by promoter methylation. Exp Cell Res 297:61–67
28. Kamitani H, Taniura S, Ikawa H, Watanabe T, Kelavkar UP, Eling TE (2001) Expression of 15-lipoxygenase-1 is regulated by histone acetylation in human colorectal carcinoma. Carcinogenesis (Oxf) 22:187–191
29. Shankaranarayanan P, Chaitidis P, Kuhn H, Nigam S (2001) Acetylation by histone acetyltransferase CREB-binding protein/p300 of STAT6 is required for transcriptional activation of the 15-lipoxygenase-1 gene. J Biol Chem 276:42753–42760
30. Kirkland JL, Dobson DE (1997) Preadipocyte function and aging: links between age-related changes in cell dynamics and altered fat tissue function. J Am Geriatr Soc 45:959–967

31. Justesen J, Stenderup K, Ebbesen EN, Mosekilde, Steiniche T, Kassem M (2001) Adipocyte tissue volume in bone marrow is increased with aging and in patients with osteoporosis. Biogerontology 2:165–171
32. Chan GK, Duque G (2002) Age-related bone loss: old bone, new facts. Gerontology 48:62–71
33. Daiscro DD Jr, Vogel RL, Johnson TE, Witherup KM, Pitzenberger SM, Rutledge SJ, Prescott DJ, Rodan GA, Schmidt A (1998) High fatty acid content in rabbit serum is responsible for the differentiation of osteoblasts into adipocyte-like cells. J Bone Miner Res 13:96–106
34. Kirkland JL, Tchkonia T, Pirtskhalava T, Han J, Karagiannides I (2002) Adipogenesis and aging: does aging make fat go MAD? Exp Gerontol 37:757–767
35. Duque G, Macoritto M, Kremer R (2004) $1,25(OH)_2D_3$ inhibits bone marrow adipogenesis in senescence accelerated mice (SAM-P/6) by decreasing the expression of peroxisome proliferator-activated receptor gamma 2 (PPARgamma2). Exp Gerontol 39:333–338
36. Lecka-Czernik B, Moerman EJ, Grant DF, Lehmann JM, Manolagas SC, Jilka RL (2002) Divergent effects of selective peroxisome proliferator-activated receptor-gamma 2 ligands on adipocyte versus osteoblast differentiation. Endocrinology 143: 2376–2384
37. Kiefer CR, Snyder LM (2000) Oxidation and erythrocyte senescence. Curr Opin Hematol 7:113–116
38. Spiteller G (2001) Lipid peroxidation in aging and age-dependent diseases. Exp Gerontol 36:1425–1457
39. Pratico D, Zhukareva V, Yao Y, Uryu K, Funk CD, Lawson JA, Trojanowski JQ, Lee VM (2004) 12/15-Lipoxygenase is increased in Alzheimer's disease: possible involvement in brain oxidative stress. Am J Pathol 164:1655–1662
40. Harats D, Shaish A, George J, Mulkins M, Kurihara H, Levkovitz H, Sigal E (2000) Overexpression of 15-lipoxygenase in vascular endothelium accelerates early atherosclerosis in LDL receptor-deficient mice. Arterioscler Thromb Vasc Biol 20:2100–2105
41. Shannon VR, Chanez P, Bousquet J, Holtzman MJ (1993) Histochemical evidence for induction of arachidonate 15-lipoxygenase in airway disease. Am Rev Respir Dis 147:1024–1028
42. Shureiqi I, Chen D, Lee JJ, Yang P, Newman RA, Brenner DE, Lotan R, Fischer SM, Lippman SM (2000) 15-LOX-1: a novel molecular target of nonsteroidal anti-inflammatory drug-induced apoptosis in colorectal cancer cells. J Natl Cancer Inst 92:1136–1142
43. Montero A, Badr KF (2000) 15-Lipoxygenase in glomerular inflammation. Exp Nephrol 8:14–19

Estrogen Receptor–Binding Fragment–Associated Antigen 9 Is a Tumor-Promoting and Prognostic Factor for Renal Cell Carcinoma

Tetsuo Ogushi,[1] Satoru Takahashi,[1] Takumi Takeuchi,[1] Tomohiko Urano,[2] Kuniko Horie-Inoue,[3] Jinpei Kumagai,[1] Tadaichi Kitamura,[1] Yasuyoshi Ouchi,[2] Masami Muramatsu,[3] and Satoshi Inoue[2,3]

Departments of [1]Urology and [2]Geriatric Medicine, Faculty of Medicine, The University of Tokyo, Hongo, Bunkyo-ku, Tokyo, Japan and [3]Research Center for Genomic Medicine, Saitama Medical School, Yamane, Hidaka-shi, Saitama, Japan

Abstract

The estrogen receptor–binding fragment–associated antigen 9 (*EBAG9*) has been identified as a primary estrogen-responsive gene in human breast cancer MCF7 cells. A high expression of EBAG9 has been observed in invasive breast cancer and advanced prostate cancer, suggesting a tumor-promoting role of the protein in malignancies. Here we show that intratumoral (i.t.) administration of small interfering RNA against EBAG9 exerted overt regression of tumors following s.c. implantation of murine renal cell carcinoma (RCC) Renca cells. Overexpression of EBAG9 did not promote the proliferation of culture Renca cells; however, the inoculated Renca cells harboring EBAG9 (Renca-EBAG9) in BALB/c mice grew faster and developed larger tumors compared with Renca cells expressing vector alone (Renca-vector). After renal subcapsular implantation, Renca-EBAG9 tumors significantly enlarged compared with Renca-vector tumors in BALB/c mice, whereas both Renca-EBAG9 and Renca-vector tumors were developed with similar volumes in BALB/c nude mice. No apparent difference was observed in specific cytotoxic T-cell responses against Renca-EBAG9 and Renca-vector cells; nonetheless, the number of infiltrating $CD8^+$ T lymphocytes was decreased in Renca-EBAG9 subcapsular tumors. Furthermore, immunohistochemical study of EBAG9 in 78 human RCC specimens showed that intense and diffuse cytoplasmic immunostaining was observed in 87% of the cases and positive EBAG9 immunoreactivity was closely correlated with poor prognosis of the patients. Multivariate analysis revealed that high EBAG9 expression was an independent prognostic predictor for disease-specific survival (P = 0.0485). Our results suggest that EBAG9 is a crucial regulator of tumor progression and a potential prognostic marker for RCC. (Cancer Res 2005; 65(9): 3700-6)

Introduction

Estrogen receptor–binding fragment associated gene 9 (*EBAG9*) is an estrogen-responsive gene that we previously identified in MCF-7 human breast carcinoma cell line using a CpG-genomic binding site cloning method (1). EBAG9 protein, whose molecular size is 32 kDa by Western blot analysis, is expressed in estrogen target organs as well as several other tissues such as brain, liver, and kidney (2). The protein expression of EBAG9 is estrogen inducible, as it has been shown in ovariectomized mice treated with 17β-estradiol administration (2). The physiologic function of EBAG9 has not been well defined, yet the molecule may be implicated in cancer pathophysiology, with several lines of evidence of the protein expression in malignancies, including breast (3), ovarian (4), prostate (5), and hepatocellular carcinomas (6). In prostate cancer (5), EBAG9 expression significantly correlated with advanced pathologic stages and high Gleason score (P = 0.0305 and P < 0.0001, respectively), suggesting the abundance of EBAG9 may relate to the progression of malignant tumors.

In the present study, we investigated whether EBAG9 expression is critical in tumor development of renal cell carcinoma (RCC). RCC that comprises the majority of kidney cancer is one of the 10 most common malignancies in industrialized countries (7). The prognosis of patients with advanced RCC is poor, as 5-year survival rate is <5% (8), and the treatment of metastatic RCC remains a difficult clinical challenge. Development of new and alternative modalities of diagnosis and therapy for RCC is a clinical requisite. We used murine syngeneic renal adenocarcinoma model of Renca cells in this study and investigated whether gene silencing or overexpression of EBAG9 influences Renca cell growth and/or *in vivo* tumorigenesis. Administration of small interfering RNA (siRNA) against EBAG9 regressed s.c. Renca tumors. The proliferation of culture Renca cells constitutively expressing EBAG9 was not basically different from control Renca cells, whereas EBAG9-expressing cells grew faster in BALB/c mice and developed larger tumors. The tumor-promoting effect of EBAG9 in Renca tumors may relate to the suppression of antitumor immunity, as i.t. $CD8^+$ T lymphocytes were reduced in renal subcapsular Renca tumors. The tumorigenic relevance of EBAG9 in Renca models further extended to clinicopathologic significance of the molecule in human RCC. EBAG9 immunoreactivity was closely correlated with poor prognosis of the patients and it was an independent prognostic predictor for disease-specific survival. Our findings show that EBAG9 is a tumor-promoting factor and a potential prognostic marker in RCC.

Materials and Methods

Reagents. Rabbit anti-EBAG9 polyclonal antibody was generated against a fusion protein of glutathione *S*-transferase and EBAG9 (2). Rabbit polyclonal antihuman CD3 antibody (DakoCytomation, Carpinteria, CA), rat antimouse CD4 (L3T4; clone RM 4-5), rat antimouse CD8a (Ly-2; 53-6.7) monoclonal antibodies (BD PharMingen, San Diego, CA), and anti–β-actin monoclonal antibody (Sigma, St. Louis, MO) were commercially purchased. Human EBAG9 cDNA was cloned into a mammalian expression vector pcDNA3 (Invitrogen, Carlsbad, CA).

Note: Supplementary data for this article are available at Cancer Research Online (http://cancerres.aacrjournals.org/).

Requests for reprints: Satoshi Inoue, Department of Geriatric Medicine, Graduate School of Medicine, The University of Tokyo, 7-3-1 Hongo, Bunkyo-ku, Tokyo 113-8655, Japan. Phone: 81-3-5800-8652; Fax: 81-3-5800-6530; E-mail: INOUE-GER@h.u-tokyo.ac.jp.

Tumor cells. Renca is a spontaneously arising murine RCC and was prepared as previously described (9, 10). Tumor cells were maintained in RPMI 1640 containing 10% FCS and antibiotics.

Mice. BALB/c mice and BALB/c *nu/nu* mice (Nisseizai, Tokyo, Japan) that were syngeneic to Renca cells were kept under specific pathogen-free conditions and fed dry food and water. All mice used for experiments were male at the age of 5 weeks.

Patients and tissue preparation. We investigated 78 tissue samples of RCC obtained from patients (14 females and 64 males) who underwent radical or partial nephrectomy at Tokyo University Hospital between 1990 and 1995. Patient information was retrieved from the review of patient charts. Staging and grading of the tumors were done according to the 1997 International Union Against Cancer tumor-node-metastasis classification and WHO histopathologic typing, respectively (11). The mean age of this population was 54 years (26-76 years) and the mean follow-up period was 60 months (2-78 months). For 32 patients with advanced tumors (pT2 or greater), adjuvant therapy was done, including immune therapy (n = 30), radiation (n = 5), and surgery for metastatic diseases in lung, colon, and pancreas (n = 8). During the follow-up period, 55 patients (70.5%) survived without evidence of disease, eight cases (10.3%) presented with tumor recurrence, and 15 cases (19.2%) died of disease. None died of other diseases.

Western blot analysis. Cells were lysed in radioimmunoprecipitation assay buffer [50 mmol/L Tris-HCl (pH 8.0), 200 mmol/L NaCl, 20 mmol/L NaF_2, 2 mmol/L EGTA, 1 mmol/L DTT, 2 mmol/L sodium vanadate, 0.5% v/v NP40 supplemented with a protease inhibitor cocktail Complete (Boehringer Manheim GmbH, Mennheim, Germany)]. Proteins were resolved by 12.5% SDS-PAGE and transferred to polyvinylidene difluoride membranes. Membranes were probed with rabbit anti-EBAG9 antibody or anti-β-actin monoclonal antibody.

Tumor regression by EBAG9 small interfering RNA. Small interfering RNA (siRNA) duplex that targets EBAG9 was generated by Dharmacon (Lafayette, CO). The target sequence of EBAG9 siRNA was 5′-AAGAAGA-UGCAGCCUGGCAAG-3′. Scramble II Duplex (Dharmacon) was used as a nontargeting control siRNA that does not possess homology with known gene targets in mammalian cells. The GC content of Scramble II Duplex was 57.9%, which was identical to that of EBAG9 siRNA.

To investigate *in vivo* silencing effect of EBAG9 siRNA in Renca tumors, i.t. injection of siRNA duplexes was done twice every week. Briefly, Renca cells (1×10^4 cells) were implanted in the flank of BALB/c mice. Tumor size was measured weekly with a micrometer in two dimensions, and tumor volume was estimated according to the formula: $(\text{smallest diameter})^2 \times$ (longest diameter). When the volumes of tumors reached 300 mm^3, siRNA duplexes (10 μg) were injected directly into tumors twice every week, along with 4 μL of GeneSilencer (Gene Therapy System, San Diego, CA) dissolved in 0.1 mL of Opti-MEM (Life Technologies, Gaithersburg, MD). Mice were sacrificed 4 weeks after treatment.

Generation of Renca cells stably expressing EBAG9. Renca cells were transfected with an expression vector pcDNA3, including human EBAG9 cDNA or vector alone using LipofectAMINE (Life Technologies). G418-resistant cells were selected and several independent clones were isolated.

Reverse transcription-PCR. Total cellular RNA of Renca cells was extracted using ISOGEN reagent (Nippon Gene, Tokyo, Japan) and first-stand cDNA was generated from 5 μg of total cellular RNA using a reverse transcriptase Omniscript RT (Qiagen, Tokyo, Japan) and random hexamers. To validate the expression of exogenous human EBAG9, reverse transcription-PCR (RT-PCR) was done using specific primers for human EBAG9 (sense 5′-GCTACACAAGATCTGCCTTT-3′ and antisense 5′-CTTCTTCATTAGCCGT-TGTG-3′). The amplification was done for 35 cycles at 62°C for annealing, using AmpliGold Taq polymerase (Perkin-Elmer, Boston, MA).

***In vivo* tumor challenge.** For s.c. implantation, transfected Renca cells (1×10^4 cells per mouse) suspended in 0.1 mL of complete medium were injected in the flank of BALB/c mice. Tumor volume was calculated weekly. In survival analyses, Renca-bearing mice were followed up for 14 weeks after implantation.

For renal subcapcular implantation, tumors cells (1×10^4 cells per mouse) suspended in 0.1 mL of complete medium were inoculated into the subcapsule of the left kidney of BALB/c wild-type and nude mice. Mice were sacrificed 25 days after implantation and tumors were excised.

Cell proliferation assay. Cells were seeded at a density of 1 to 3 $\times 10^5$ cells per dish into 10-cm dishes and hemocytometer counting was done every 2 days. Doubling time during exponential growth was determined by a formula: [incubation time (h) $\times \log_{10}2$] / [$\log_{10}$(cell number at sampling period) − $\log_{10}$(plating cell number)] (12).

Proliferation assays were done using the 2-(2-methoxy-4-nitrophenyl)-3-(4-nitrophenyl)-5-(2,4-disulfophenyl)-2*H* tetrazolium monosodium salt (WST-8) reagent (Nacalai, Kyoto, Japan; ref. 13). The assay is based on the conversion of the 3-(4,5-dimethylthiazol-2-yl)-2,5-diphenyltetrazolium bromide (MTT)-like tetrazolium salt WST-8 to a water-soluble formazan by metabolically active cells and provides a quantitative determination of viable cells. Cells were seeded in 96-well plates at an initial density of 625 to 5,000 cells per well. At 1 hour after inoculation, cells were transfected with either EBAG9 siRNA or Scramble II Duplex (100 ng per well) using GeneSilencer reagent (Gene Therapy Systems). Assays were done on days 0, 2, and 4. For cells cultured up to day 4, medium was once exchanged on day 2. Spectrophotometric absorbance at 450 nm (for formazan dye) was measured with absorbance at 620 nm for reference.

Cytotoxicity assay. Renca-EBAG9 or Renca-vector cells were used as target cells. Splenocytes of Renca-bearing BALB/c mice were stimulated for 5 days *in vitro* with irradiated Renca cells at a splenocyte/tumor cell ratio of 20:1 in the presence of 1,000 IU/mL interleukin-2 and used as effector CTLs. Target cells were incubated with effector CTLs at various E/T ratios in a final volume of 200 μL for 18 hours at 37°C. Lactate dehydrogenase release from cells with a damaged membrane was examined using CytoTox-ONE Reagent (Promega, Madison, WI) and fluorescence was measured with an excitation wavelength of 560 nm and an emission wavelength of 590 nm. Experiments were done in triplicate.

Immunohistochemistry. Immunohistochemical studies were done using the streptavidin-biotin amplification method with horseradish peroxidase detection. Paraffin sections of tumors were blocked in 0.3% H_2O_2 (30 minutes) and in 10% FCS (30 minutes), incubated overnight with specific antibodies against CD3, CD4, or CD8a for Renca tumors (1:20 dilution), or with purified rabbit anti-EBAG9 antibody for human RCC (1:40 dilution). Sections were incubated with biotinylated rabbit antirat immunoglobulin G or antirabbit EnVison$^+$ reagent (DakoCytomation), developed by diaminobenzidine (Sigma), and counterstained with hematoxylin (Sigma). Negative controls were done for each slide, using nonimmune immunoglobulin G.

In Renca experiments, numbers of tumor-infiltrating lymphocytes (TILs) positive for CD3, CD4, or CD8 expression were microscopically examined in the high-power field of view at a magnification of 400× (14). BALB/c mouse spleen specimen was used as a positive control.

In RCC examination, immunoreactivity scores of EBAG9 expression were determined by two pathologists according to percentages of positive cells. Human breast cancer section (DakoCytomation) was used as a positive control. Positivity was 0% to 4% for immunoreactivity score of 0 (negative), 5% to 24% for a score of 1+, 25% to 49% for a score of 2+, and 50% to 100% for a score of 3+. Sections that had ≥25% positive cells but apparent lower intensity compared with positive controls were scored as immunoreactivity score of 1+. Immunoreactivity scores of 1+, 2+, and 3+ were defined as positive staining. If immunoreactivity scores were different between two pathologists, the average immunoreactivity score was adopted. If several types of histology were included in one section, immunoreactivity score of predominant histology was used.

Statistical analyses. Comparisons between different groups of Renca samples were analyzed with nonparametrical Mann-Whitney U test. The associations between EBAG9 immunoreactivity and clinicopathologic characteristics were evaluated by Student's t test or Fisher's exact probability test. Disease-specific survival was computed by Kaplan-Meier method and the curves were compared by log-rank test. Multivariate analysis of prognostic factors was done using Cox proportional hazard regression model. Computations were done with the StatView 5.0J software (SAS Institute, Inc., Cary, NC). All Ps are two sided and evaluated as significant if $P < 0.05$.

Results

Gene silencing of EBAG9 suppressed *in vivo* tumor growth of Renca cells. To determine the role of EBAG9 in tumor growth of renal cancer cells, we investigated the effects of synthesized siRNA duplexes targeting EBAG9 on s.c. tumor models of Renca cells implanted in syngeneic BALB/c mice. Intratumoral injection of EBAG9 siRNA reduced the protein levels of endogenous EBAG9 compared with the levels of EBAG9 in parental Renca cells or in the Renca tumor treated with control scrambled siRNA duplexes (Fig. 1*A*). Under the treatment of scrambled siRNA, s.c. implanted Renca cells developed prominent tumors, whereas the injection of EBAG9 siRNA suppressed tumor growth of Renca cells (Fig. 1*B* and *C*). After 4-week treatments, the volume of tumors with EBAG9 siRNA treatment was significantly smaller than that with scrambled siRNA (3,854 ± 665 versus 6,315 ± 1,053 mm^3, $n = 5$; $P = 0.0472$). We infer that tumor growth is modulated by EBAG9 expression, implicating EBAG9 as a tumor-promoting factor in renal carcinoma.

Generation of Renca cells stably expressing EBAG9. To explore whether constitutive EBAG9 expression influences tumor growth, we generated Renca cells stably expressing human EBAG9. We selected two Renca-EBAG9 cell clones 3 and 4 that express human EBAG9 mRNA as confirmed by RT-PCR using human EBAG9–specific primers (Fig. 2*A*, *top*). The amounts of EBAG9 proteins in Renca-EBAG9 cells were ~2.0 fold increased compared with those in parental Renca cells and Renca-vector cell clones 1 and 2, which were transfected with pcDNA3 empty vector (Fig. 2*A*, *bottom*). In terms of cell growth rate, doubling time of culture Renca-EBAG9 cells was not significantly different from that of Renca-vector cells (Fig. 2*B*). Proliferation of Renca cells was further analyzed by a colorimetric MTT-like assay using a tetrazolium monosodium salt WST-8 that is converted to a water-soluble formazan by metabolically active cells (Fig. 2*C*). Neither EBAG9 overexpression nor RNA interference against EBAG9 did not significantly influence the growth of Renca cells. Moreover, EBAG9 overexpression did not influence the incorporation of bromodeoxyuridine in culture Renca cells (data not shown). The results suggest that stable expression of EBAG9 itself does not accelerate the proliferation of culture tumor cells.

EBAG9 promotes *in vivo* tumor growth of Renca cells. In spite of little difference of propagation abilities between Renca-EBAG9 cells and Renca-vector cells in culture, Renca-EBAG9 cells s.c. implanted into BALB/c mice developed >4-fold larger tumors compared with Renca-vector cells at 4 weeks after inoculation (Fig. 3*A* and *B*). Mean tumor volumes at 4 weeks were 1,712 ± 506 mm^3 for Renca-EBAG9 cell clones 3 and 4 versus 366 ± 110 mm^3 for Renca-vector cell clones 1 and 2 ($P = 0.0055$; Fig. 3*B*).

In terms of prognosis of mice harboring Renca tumors, 23.5% of mice with Renca-vector cells ($n = 17$) survived on day 100 after tumor challenge whereas only 5.6% of mice with Renca-EBAG9 cells ($n = 18$) survived at the same period (Fig. 3*C*; $P = 0.0412$ by log-rank test). Systemic metastases, including tumor dissemination into peritoneum and distant metastases of lung and liver, were reasons for death in all deceased cases.

EBAG9 suppresses host immune surveillance. To determine whether aberrant EBAG9 expression in Renca cells affects the local immune responses in tumors, we implanted Renca-EBAG9 cells or Renca-vector cells under the renal capsule of BALB/c mice and immunodeficient BALB/c nude mice. Both Renca cell lines formed macroscopic tumors in all of the cancer-bearing hosts by day 25 (Fig. 4*A*). In conventional BALB/c mice, Renca-EBAG9 tumors grew significantly larger compared with Renca-vector tumors (Fig. 4*A* and *B*). Mean volumes of tumors on day 25 in BALB/c mice were 856 ± 162 mm^3 ($n = 19$) for Renca-EBAG9 clones 3 and 4 versus 149 ± 59 mm^3 ($n = 18$) for Renca-vector clones 1 and 2 (Fig. 4*B*; $P < 0.0001$). In immunodeficient BALB/c nude mice, both Renca-vector cells and Renca-EBAG9 cells developed extensive tumors compared with tumors in BALB/c mice and there was no significant difference in tumor volumes between Renca-vector cells and Renca-EBAG9 cells (Fig. 4*A* and *B*). Mean volumes of tumors on day 25 in BALB/c nude mice were 2,215 ± 227 mm^3 ($n = 18$) for Renca-EBAG9 clones 3 and 4 versus 1,802 ± 240 mm^3 ($n = 23$) for Renca-vector clones 1 and 2 (Fig 4*B*; $P = 0.118$). These results may suggest that aberrant EBAG9 expression in Renca cells hampers a local primary immune response

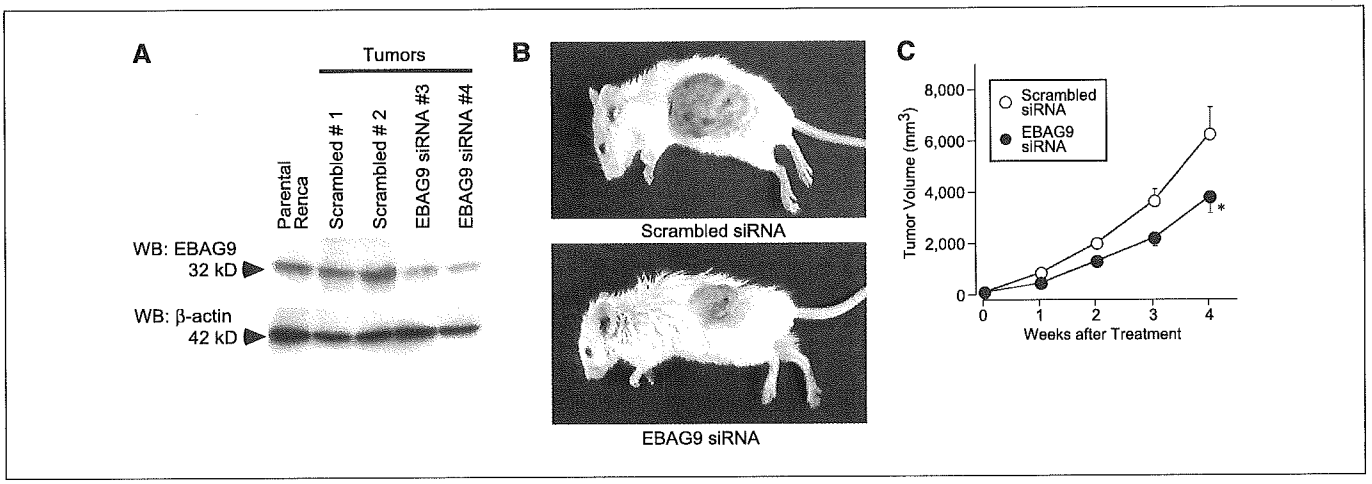

Figure 1. Expression of EBAG9 siRNA suppresses tumor growth derived from murine renal cell carcinoma Renca cells in BALB/c mice. S.c. primary Renca tumors were established by midflank injections of 10,000 tumor cells and i.t. injections of either control scrambled siRNA or EBAG9 siRNA duplexes together with a transfection reagent GeneSilencer were done twice a week in five mice per group when the initial tumor volumes reached 300 mm^3. Mice were sacrificed after 4 weeks of siRNA administration and tumors were homogenized for protein extraction. *A*, Western blot analysis of lysates from *in vitro* culture Renca cells and tumor samples expressing either control scrambled siRNA or EBAG9 siRNA. *B*, representative mice after 4 weeks of siRNA treatment. *Top*, mouse treated with control scrambled siRNA. *Bottom*, mouse treated with EBAG9 siRNA. *C*, tumor volume in EBAG9 siRNA–treated mice ($n = 5$) is reduced compared with control mice ($n = 5$). *, $P < 0.05$ at 4 weeks (EBAG9 siRNA versus scrambled siRNA).

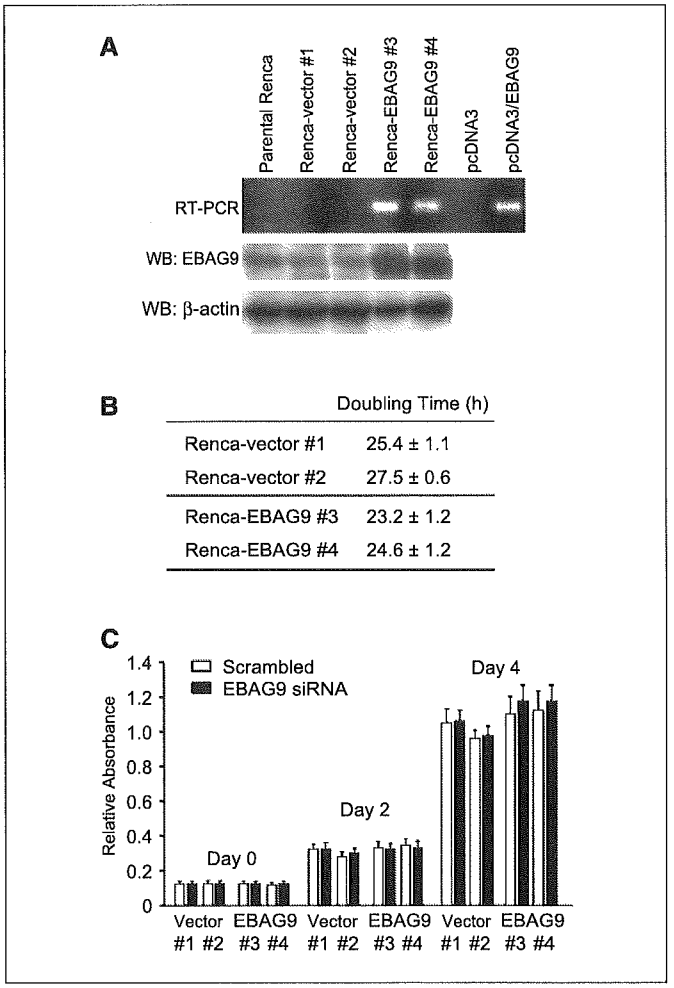

Figure 2. Overexpression of EBAG9 in Renca cells does not accelerate culture cell growth. *A*, RT-PCR analysis and Western blot analysis of Renca cells stably expressing human EBAG9 (Renca-EBAG9) or empty vector (Renca-vector). *Top*, human EBAG9 mRNA is expressed in clones 3 and 4 of Renca-EBAG9 cells. Empty pcDNA3 vector was used as a negative control and pcDNA3 including EBAG9 cDNA as a positive control. *Bottom*, EBAG9 protein is overexpressed in Renca-EBAG9 clones compared with Renca-vector clones or parental Renca cells. *B*, doubling time of culture Renca cells. The numbers of cells in the exponential growth were counted every 2 days and doubling time was calculated according to a formula as described in Materials and Methods ($n = 5$ for each). *C*, proliferative assay using WST-8 tetrazolium salt. Cells seeded into 96-well plates were transfected with control scrambled siRNA or EBAG9 siRNA duplexes (100 ng per well) and cell proliferation was evaluated on days 0, 2, and 4 ($n = 3$ for each). Absorbance at 450 nm (for formazan dye) was measured with absorbance at 620 nm for reference.

that retards the growth of tumors rather than potentiates the intrinsic tumorigenicity of the tumor cells.

To investigate whether the progression of Renca-EBAG9 tumors depends on a reduced sensitivity of the cells to tumor-specific CTLs, we did cytotoxicity assays. Effector CTLs were derived from splenocytes of Renca-bearing BALB/c mice, after a 5-day restimulation with Renca cells in the presence of interleukin-2. (Fig. 4*C*). Renca-EBAG9 cells and Renca-vector cells were equally lysed by tumor-specific CTLs, suggesting that EBAG9 expression itself does not affect the sensitivity of Renca cells to CTL lysis.

To assess whether EBAG9 modulates the subtype-specific reactivity of T lymphocytes against tumors, we examined the numbers of TILs in renal subcapsular Renca tumors developed in BALB/c mice (Fig. 4*D*). No significant differences in numbers of $CD3^+$ and $CD4^+$ T cells were observed between Renca-vector and Renca-EBAG9 tumors, whereas the number of $CD8^+$ T cells in Renca-EBAG9 tumors was significantly decreased compared with that in Renca-vector tumors ($P < 0.05$).

Expression of EBAG9 protein in human renal cell carcinoma tumors. The finding that EBAG9 modulated the growth of Renca tumors led us to the notion whether the molecule contributes to the progression of RCC in human tissues. EBAG9 expression was evaluated immunohistochemically in 78 RCC whole tissue specimens including normal lesions. In noncarcinomatous lesions, a weak and scattered immunostaining of EBAG9 was observed in the cytoplasm of the mesangial cells (Fig. 5*A*) as well as on the luminal surface of the renal tubular

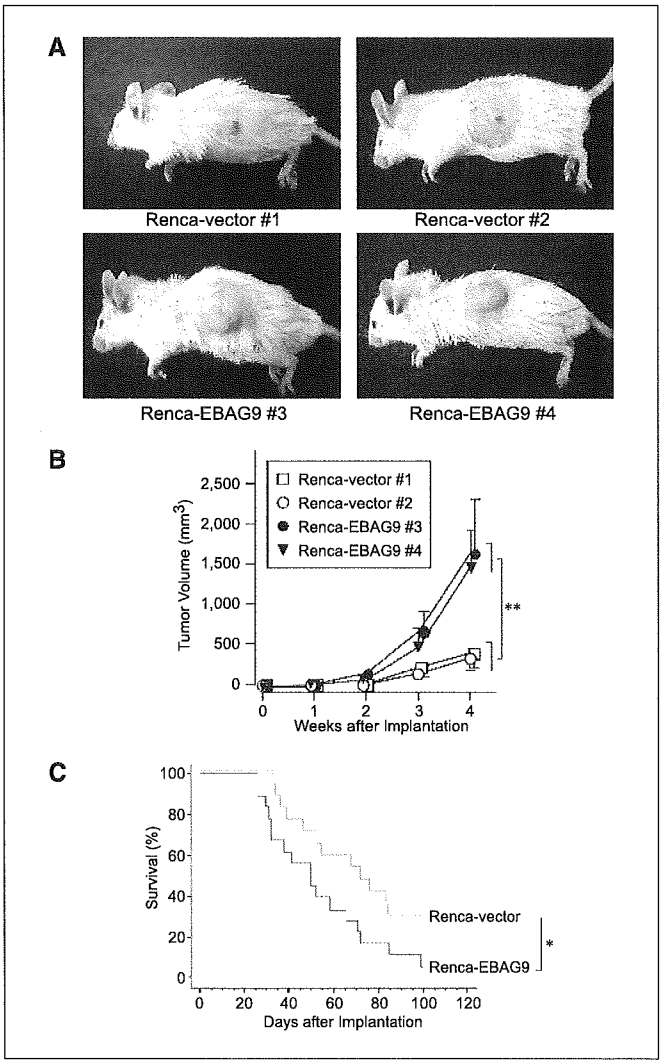

Figure 3. Renca cells stably expressing EBAG9 develop large tumors in BALB/c mice. *A*, representative mice 4 weeks after the inoculation of tumor cells. *B*, volumes of tumors derived from Renca-EBAG9 cells are significantly larger compared with Renca-vector cells in BALB/c mice. S.c. primary tumors were established by midflank injections of 10,000 tumor cells. **, $P < 0.01$ at 4 weeks (Renca-EBAG9 versus Renca-vector). Renca-vector 1, $n = 16$; Renca-vector 2, $n = 6$; Renca-EBAG9 3, $n = 6$; Renca-EBAG9 4, $n = 8$. *C*, poorer prognosis of mice inoculated with Renca-EBAG9 cells compared with mice with Renca-vector cells. Disease-specific survival on day 100: $P = 0.0412$ (Renca-EBAG9 versus Renca-vector). Renca-vector 1, $n = 9$; Renca-vector 2, $n = 8$; Renca-EBAG9 3, $n = 8$; Renca-EBAG9 4, $n = 10$.

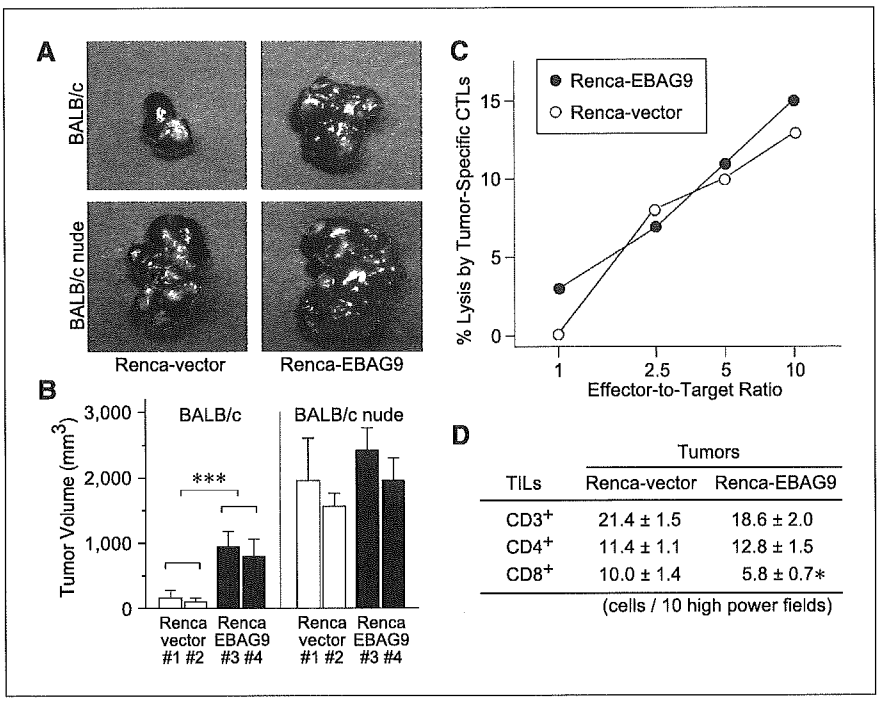

Figure 4. EBAG9 overexpression promotes renal subcapsular tumor growth by Renca cells in wild-type BALB/c mice. *A*, representative tumors 25 days after the inoculation of tumor cells (10,000 cells). *B*, volumes of Renca-EBAG9 tumors are larger than Renca-vector tumors in BALB/c mice, whereas no significant difference of tumor volumes between Renca-vector and Renca-EBAG9 in BALB/c nude mice. **, $P < 0.0001$ on day 25 (Renca-EBAG9 versus Renca-vector). Renca-vector 1, $n = 12$; Renca-vector 2, $n = 11$; Renca-EBAG9 3, $n = 9$; Renca-EBAG9 4, $n = 9$. *C*, lysis of Renca-EBAG9 and Renca-vector cells by tumor-specific CTLs. Splenocytes from Renca-bearing mice were cultured with Renca cells at a ratio of 20:1 pulsed with interleukin-2 (1,000 units/mL) for 5 days. Lactate dehydrogenase release from cells with a damaged membrane was examined using CytoTox-ONE Reagent and fluorescence was measured with an excitation wavelength of 560 nm and an emission wavelength of 590 nm. *D*, numbers of tumor infiltrating-lymphocytes positive for CD3, CD4, or CD8 immunostaining were microscopically examined in the high-power field of view at a magnification of 400×. BALB/c mouse spleen specimen was used as a positive control. *, $P < 0.05$ (Renca-EBAG9 versus Renca-vector).

cells (data not shown). The levels of EBAG9 expression in normal renal tissues corresponded to immunoreactivity score of 0. In RCC tumors, 10 of 78 cases (13%) had negative immunoreactivity of EBAG9, whereas 68 of cases (87%) showed EBAG9 positivity. With regard to EBAG9-positive RCC tumors, the cancer cells generally retain intense and diffuse staining patterns in the cytoplasm or on the membrane (Fig. 5*B*, *C*, and *D*). The levels of EBAG9 positivity were immunoreactivity score of 1+ for 18 RCC tumors (23%), 2+ for 31 tumors (40%), and 3+ for 19 tumors (24%). With respect to RCC histology, clear cell tumors displayed an intense membrane staining as well as a diffuse cytoplasmic staining of EBAG9 (Fig. 5*B*; immunoreactivity score, 2+). Sarcomatoid tumors showed an intense and frequent cytoplasmic immunoreactivity (Fig. 5*C*; immunoreactivity score, 3+). Lung metastatic tumors showed the highest EBAG9 staining, predominantly in the cytoplasm (Fig. 5*D*; immunoreactivity score, 3+).

A significant association between EBAG9 immunoreactivity and clinicopathologic variables was observed in RCC patients (Supplementary Table 1). EBAG9 positivity (immunoreactivity score, >1+) was significantly correlated with advanced pathologic tumor stages, positivity of vascular infiltration, and nonclear cell histology ($P = 0.0017$, $P = 0.0109$, and $P = 0.0126$, respectively).

In Kaplan-Meier analysis of the RCC patients, those in which the tumor had high EBAG9 immunoreactivity (immunoreactivity score, 3+) showed a shorter disease-specific survival (Fig. 6) compared with patients showing low or negative EBAG9 immunoreactivity (immunoreactivity score, 0-2+). The 5-year disease-specific survival in cases with EBAG9 immunoreactivity score of 3+ was 55%, whereas 91.2% of patients with low or negative EBAG9 immunoreactivity were alive during the same period.

In univariate Cox proportional hazards analysis for a 5-year disease-specific survival, established prognostic factors including infiltration, pathologic stage, and metastatic status are the most significant univariate variables of survival (Supplementary Table 2; $P < 0.0001$ for all). Lower EBAG9 immunoreactivity as well as negativity of lymph node status or vascular infiltration are also involved in significant univariate survival predictors ($P = 0.0007$, 0.0002, and 0.0003, respectively). In multivariate Cox proportional hazards analysis, negative metastatic status is the most significant predictor of survival (Supplementary Table 3; $P < 0.001$; relative risk, 42.53) Notably, high EBAG9 immunoreactivity is associated with disease-specific death in multivariate analysis ($P = 0.0485$; relative risk, 5.09). These results indicate that high immunoreactivity of EBAG9 is a potential poor prognostic variable in RCC patients.

Discussion

The present study shows the first evidence regarding a tumor-promoting role of EBAG9 *in vivo*. We showed that Renca tumors overexpressing EBAG9 had a much aggressive phenotype with poorer prognosis compared with Renca tumors expressing empty vector, although the effects of EBAG9 on culture cell proliferation was relatively minimal. EBAG9 immunoreactivity was detected in most of human RCC samples and high amounts of EBAG9 protein may associate with poor prognosis of the patients. Our findings suggest that EBAG9 is a tumor-promoting factor in RCC yet does not function as an essential oncogene by itself. The present results lead us to the notion that EBAG9 potentiates tumor growth by altering tumor microenvironment.

Decreased local immune responses may be one of the critical mechanisms that change tumor microenvironment. In antitumor immunity, T lymphocyte–mediated immune surveillance is thought a principal host defense mechanism (15). Although tumors such as RCC are immunogenic and could be targeted by tumor-specific CTL or natural killer cells, antitumor immune

reactions are not completely effective to reject tumor cells so that tumors continue to grow progressively (16). In our cytotoxicity assay, there was no significant difference of CTL lysis between Renca-EBAG9 and Renca-vector cells, suggesting that overexpression of EBAG9 may not particularly alter the presentation of tumor-associated antigens or the levels of MHC class I molecule expression. In TIL assay, however, $CD8^+$ T cells seemed specifically reduced by aberrant EBAG9 expression. We suspect that generation of immunosuppressive factors or apoptosis activation may result in the reduction of $CD8^+$ TIL, leading to hamper antitumor immunity.

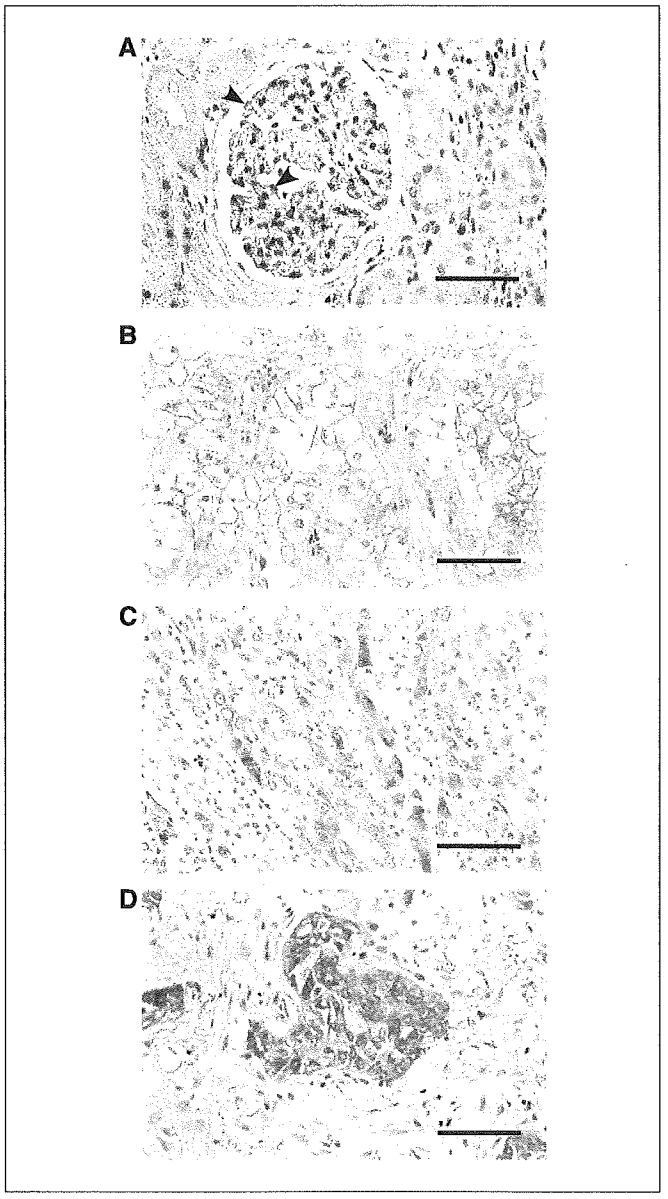

Figure 5. EBAG9 immunostaining in human kidney and renal cell carcinoma specimens. *A*, normal kidney (immunoreactivity score, 0). EBAG9 is weakly expressed in the mesangial cells (*arrowheads*). *B*, clear cell carcinoma (immunoreactivity score, 1+). EBAG9 is immunostained predominantly on the cell membrane in cancerous regions. *C*, spindle cell carcinoma (immunoreactivity score, 3+). Intense immunostaining of EBAG9 is observed in the cytoplasm of sarcomatoid cancerous regions. *D*, lung metastatic tumors (immunoreactivity score, 3+). Intense immunoreactivity of EBAG9 is observed in metastatic tumors with high immunoreactivity scores. *Bars*, 50 μm.

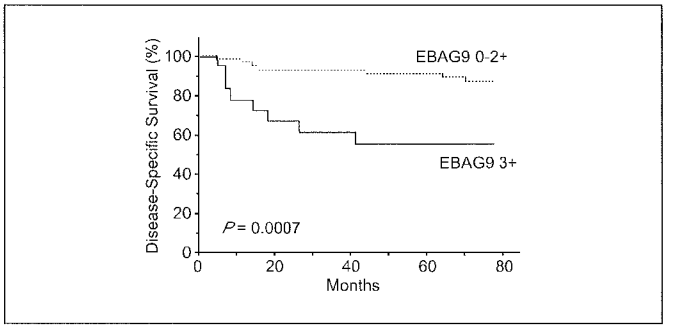

Figure 6. Association of immunocytochemical staining for EBAG9 with disease-specific survival of 78 RCC patients. Five-year disease-specific survival of the patients with high EBAG9 immunoreactivity (immunoreactivity score, 3+; $n = 19$) was significantly worse than the patients with immunoreactivity scores of 0-2+ ($n = 59$; 55% versus 91%, $P = 0.0007$, by log-rank test).

The alteration in cell surface glycosylation could be implicated in the modulation of tumor microenvironments (17, 18). It has been recently shown that tumor-associated ganglioside expression in human RCC cells suppresses nuclear factor-κB activation in T cells and mediates T-cell apoptosis (19, 20). RCC display increased levels of gangliosides including GM2, GM1, and GD1a (21) as well as several disialogangliosides (22), which may inhibit the function of antigen-presenting cells (23) or modulate tumor vascularization (24). It has been recently shown that tumor-associated *O*-linked glycan antigens Tn and TF were expressed in transfected cells expressing RCAS1 (receptor-binding cancer antigen expressed on SiSo cells; ref. 25), whose cDNA has been found to be a homologue of EBAG9 (26).

Another possible explanation is that EBAG9 may stimulate angiogenesis by up-regulating growth factors or cytokines. There are literatures that suggest that vascular endothelial growth factor (VEGF) could be involved in RCC tumor progression. Mutations of the von Hippel-Lindau tumor suppressor gene, which are often observed in hereditary RCC and sporadic clear cell RCC, result in overproduction of VEGF through a mechanism involving hypoxia-inducible factor α (27, 28). It has been recently shown that VEGF interferes with the development of T cells at pathologically relevant concentrations *in vivo* (29); thus, the growth factor may contribute to tumor-associated immune deficiencies.

It has been generally accepted that tumor cells may escape from immune surveillance by expressing the EBAG9 homologue RCAS1, which targets RCAS1 receptor–expressing immune cells and induces apoptosis (26). Nakashima et al. identified the RCAS1 cDNA through expression cloning using the 22-1-1 monoclonal antibody that they originally generated (30). Engelsberg et al. recently showed, however, that the 22-1-1 epitope was distinct from the products encoded by RCAS1 cDNA, because the RCAS1 protein was not recognized by the 22-1-1 antibody, whereas the 22-1-1 antibody recognized the tumor-associated *O*-linked glycan antigens (25). They showed that their raised polyclonal antibody recognized a ~35-kDa protein, consistent with the immunoblotting results using our polyclonal antibody. On the contrary, the putative RCAS1 protein recognized by the 22-1-1 antibody was identified as an ~80-kDa membrane molecule expressed on human uterine cancer cells (26, 30). Although there are a number of publications concerning RCAS1 in cancers from the point of view as the 22-1-1 antigen, we consider that a pathophysiologic role of EBAG9 in tumor immunology needs to be properly evaluated. The present article may provide new insights into an EBAG9-mediated *in vivo* function in cancer progression.

We have previously reported that the immunoreactivity of EBAG9 was mainly observed in the cytoplasm of normal epithelial cells with a granular staining pattern, or particularly in perinuclear regions (3, 5). In carcinoma tissues, an intense staining of the cell surface could be also observed such as in prostate cancer or hepatocellular carcinoma. The expression of RCAS1 immunoreactivity recognized by antibodies against recombinant RCAS1 was localized to perinuclear structures, suggesting that the protein is predominantly distributed in the Golgi system (25). Given that EBAG9 is a Golgi-predominant protein that could be trafficking from the perinuclear regions to the cell surface membrane, it is likely that EBAG9 immunoreactivity could be observed in both cytoplasm and cell surface of cancerous tissues with the abundant expression of EBAG9. Notably, EBAG9 immunoreactivity in RCC with advanced stages such as sarcomatoid or metastatic tumors was cytoplasmic predominant (Fig. 5*C* and *D*). Further studies using confocal or electron microscopic examination may elucidate the dynamic distribution of EBAG9.

As we showed that there are several types of cancer that intensely express EBAG9 and the expression levels of EBAG9 may relate to advanced tumor grades (3–6), it is likely that the tumor-promoting effect of EBAG9 is a general event in malignancies regardless of their estrogen dependency. We also observed the lack of association between sex and EBAG9 expression in human RCC in our clinicopathologic study (Supplementary Table 1). Thus, EBAG9 could be a therapeutic target for various tumors constitutively expressing the molecule.

In summary, we show that EBAG9 is a tumor-promoting factor in both murine Renca RCC and human RCC. We propose that EBAG9 immunoreactivity is a new potential biomarker for prognosis of RCC and a treatment modality targeting EBAG9 will provide a novel therapeutic option for advanced RCC.

Acknowledgments

Received 9/28/2004; revised 2/15/2005; accepted 2/25/2005.

Grant support: Ministry of Health, Labor and Welfare Japan, the Ministry of Education, Culture, Sports, Science and Technology Japan.

The costs of publication of this article were defrayed in part by the payment of page charges. This article must therefore be hereby marked *advertisement* in accordance with 18 U.S.C. Section 1734 solely to indicate this fact.

We thank T. Suzuki for her technical assistance.

References

1. Watanabe T, Inoue S, Hiroi H, Orimo A, Kawashima H, Muramatsu M. Isolation of estrogen-responsive genes with a CpG island library. Mol Cell Biol 1998;18:442–9.
2. Tsuchiya F, Ikeda K, Tsutsumi O, et al. Molecular cloning and characterization of mouse EBAG9, homolog of a human cancer associated surface antigen: expression and regulation by estrogen. Biochem Biophys Res Commun 2001;284:2–10.
3. Suzuki T, Inoue S, Kawabata W, et al. EBAG9/RCAS1 in human breast carcinoma: a possible factor in endocrine-immune interactions. Br J Cancer 2001;85:1731–7.
4. Akahira JI, Aoki M, Suzuki T, et al. Expression of EBAG9/RCAS1 is associated with advanced disease in human epithelial ovarian cancer. Br J Cancer 2004;90: 2197–202.
5. Takahashi S, Urano T, Tsuchiya F, et al. EBAG9/RCAS1 expression and its prognostic significance in prostatic cancer. Int J Cancer 2003;106:310–5.
6. Aoki T, Inoue S, Imamura H, et al. EBAG9/RCAS1 expression in hepatocellular carcinoma: correlation with tumour dedifferentiation and proliferation. Eur J Cancer 2003;39:1552–61.
7. Landis SH, Murray T, Bolden S, Wingo PA. Cancer statistics. CA Cancer J Clin 1999;49:8–31.
8. Moch H, Gasser T, Amin MB, Torhorst J, Sauter G, Mihatsch MJ. Prognostic utility of the recently recommended histologic classification and revised TNM staging system of renal cell carcinoma: a Swiss experience with 588 tumors. Cancer 2000;89:604–14.
9. Takeuchi T, Ueki T, Sasaki Y, et al. Th2-like response and antitumor effect of anti-interleukin-4 mAb in mice bearing renal cell carcinoma. Cancer Immunol Immunother 1997;43:375–81.
10. Nishimatsu H, Takeuchi T, Ueki T, et al. CD95 ligand expression enhances growth of murine renal cell carcinoma *in vivo*. Cancer Immunol Immunother 1999;48:56–61.
11. Gelb AB. Renal cell carcinoma: current prognostic factors. Union Internationale Contre le Cancer (UICC) and the American Joint Committee on Cancer (AJCC). Cancer 1997;80:981–6.
12. Dawson M. Initiation and maintenance of cultures. In: Bulter M, Dawson M, editors. Cell culture labfax. Oxford: BIOS Scientific; 1992. p. 25–42.
13. Miyamoto T, Min W, Lillehoj HS. Lymphocyte proliferation response during *Eimeria tenella* infection assessed by a new, reliable, nonradioactive colorimetric assay. Avian Dis 2002;46:10–6.
14. Schumacher K, Haensch W, Roefzaad C, Schlag PM. Prognostic significance of activated CD8(+) T cell infiltrations within esophageal carcinomas. Cancer Res 2001;61:3932–6.
15. Shankaran V, Ikeda H, Bruce AT, et al. IFNγ and lymphocytes prevent primary tumour development and shape tumour immunogenicity. Nature 2001;410: 1107–11.
16. Pawelec G. Immunotherapy and immunoselection: tumour escape as the final hurdle. FEBS Lett 2004;567: 63–6.
17. Springer GF. Immunoreactive T and Tn epitopes in cancer diagnosis, prognosis, and immunotherapy. J Mol Med 1997;75:594–602.
18. Hakomori S. Glycosylation defining cancer malignancy: new wine in an old bottle. Proc Natl Acad Sci U S A 2002;99:10231–3.
19. Kudo D, Rayman P, Horton C, et al. Gangliosides expressed by the renal cell carcinoma cell line SK-RC-45 are involved in tumor-induced apoptosis of T cells. Cancer Res 2003;63:1676–83.
20. Thornton MV, Kudo D, Rayman P, et al. Degradation of NF-κ B in T cells by gangliosides expressed on renal cell carcinomas. J Immunol 2004;172:3480–90.
21. Ritter G, Livingston PO. Ganglioside antigens expressed by human cancer cells. Semin Cancer Biol 1991; 2:401–9.
22. Ito A, Levery SB, Saito S, Satoh M, Hakomori S. A novel ganglioside isolated from renal cell carcinoma. J Biol Chem 2001;276:16695–703.
23. Caldwell S, Heitger A, Shen W, Liu Y, Taylor B, Ladisch S. Mechanisms of ganglioside inhibition of APC function. J Immunol 2003;171:1676–83.
24. Manfredi MG, Lim S, Claffey KP, Seyfried TN. Gangliosides influence angiogenesis in an experimental mouse brain tumor. Cancer Res 1999;59:5392–7.
25. Engelsberg A, Hermosilla R, Karsten U, Schulein R, Dorken B, Rehm A. The Golgi protein RCAS1 controls cell surface expression of tumor-associated O-linked glycan antigens. J Biol Chem 2003;278:22998–3007.
26. Nakashima M, Sonoda K, Watanabe T. Inhibition of cell growth and induction of apoptotic cell death by the human tumor-associated antigen RCAS1. Nat Med 1999; 5:938–42.
27. Gnarra JR, Zhou S, Merrill MJ, et al. Post-transcriptional regulation of vascular endothelial growth factor mRNA by the product of the VHL tumor suppressor gene. Proc Natl Acad Sci U S A 1996;93: 10589–94.
28. Turner KJ, Moore JW, Jones A, et al. Expression of hypoxia-inducible factors in human renal cancer: relationship to angiogenesis and to the von Hippel-Lindau gene mutation. Cancer Res 2002;62:2957–61.
29. Ohm JE, Gabrilovich DI, Sempowski GD, et al. VEGF inhibits T-cell development and may contribute to tumor-induced immune suppression. Blood 2003;101: 4878–86.
30. Sonoda K, Nakashima M, Kaku T, Kamura T, Nakano H, Watanabe T. A novel tumor-associated antigen expressed in human uterine and ovarian carcinomas. Cancer 1996;77:1501–9.

Estrogen-Responsive Finger Protein as a New Potential Biomarker for Breast Cancer

Takashi Suzuki,[1] Tomohiko Urano,[3] Tohru Tsukui,[4] Kuniko Horie-Inoue,[4] Takuya Moriya,[1] Takanori Ishida,[2] Masami Muramatsu,[4] Yasuyoshi Ouchi,[3] Hironobu Sasano,[1] and Satoshi Inoue[3,4]

Abstract

Purpose: Estrogen-responsive finger protein (Efp) is a member of RING finger-B box-Coiled Coil family and is also a downstream target of estrogen receptor α. Previously, Efp was shown to mediate estrogen-induced cell growth, which suggests possible involvement in the development of human breast carcinomas. In this study, we examined expression of Efp in breast carcinoma tissues and correlated these findings with various clinicopathologic variables.

Experimental Design: Thirty frozen specimens of breast carcinomas were used for immunohistochemistry and laser capture microdissection/real-time PCR of Efp. Immunohistochemistry for Efp was also done in 151 breast carcinoma specimens fixed with formalin and embedded in paraffin wax.

Results: Efp immunoreactivity was detected in breast carcinoma cells and was significantly associated with the mRNA level (n = 30). Efp immunoreactivity was positively associated with lymph node status or estrogen receptor α status and negatively correlated with histologic grade or 14-3-3σ immunoreactivity (n = 151). Moreover, Efp immunoreactivity was significantly correlated with poor prognosis of breast cancer patients, and multivariate analyses of disease-free survival and overall survival for 151 breast cancer patients showed that Efp immunoreactivity was the independent marker.

Conclusions: Our data suggest that Efp immunoreactivity is a significant prognostic factor in breast cancer patients. These findings may account for an oncogenic role of Efp in the tumor progression of breast carcinoma.

Breast cancer is the most common type of cancer and continues to be the most frequent cause of cancer-related deaths in women in the Western world. Whether or not human primary breast cancers are estrogen dependent is a critical factor that determines patient prognosis and availability of antiestrogenic endocrine therapy (1). Two thirds of breast carcinomas are positive for estrogen receptor α (ERα) and a great majority of these tumors initially respond to antiestrogens such as tamoxifen and aromatase inhibitors. However, it is also true that these ERα-positive breast carcinomas frequently acquire resistance to endocrine therapy, although ERα remains to be expressed (1, 2). The molecular mechanisms through which breast carcinomas become hormone-refractory are still largely unclear.

Identification and functional studies of ERα target molecules may provide a clue for understanding the mechanism that alters tumor phenotypes. We have previously isolated estrogen-responsive finger protein (Efp), which is a member of RING finger-B box-Coiled Coil family (3). Efp also is one of the downstream targets of ERα (3–6). Efp-deficient mice displayed underdeveloped uteri and reduced estrogen responsiveness (7), and therefore, Efp is considered to be essential for estrogen-dependent proliferation. It has also been shown that Efp promotes the growth of breast tumor by functioning as a ubiquitin ligase (E3) that targets the negative cell cycle checkpoint 14-3-3σ (8).

Expression of Efp was previously reported in breast carcinoma tissues at mRNA (5) and protein levels (9). However, information on the expression of Efp in human breast carcinoma tissues is still very limited, and the biological significance of Efp remains unclear at this juncture. Therefore, in this study, we examined expression of Efp in 30 cases of breast carcinoma tissues using immunohistochemistry and laser capture microdissection/real-time PCR. We subsequently examined immunolocalization of Efp in 151 cases of human breast carcinoma tissues and correlated these findings with various clinicopathologic factors including clinical outcome of the patients.

Authors' Affiliations: Departments of [1]Pathology and [2]Surgery, Tohoku University School of Medicine, Aoba-ku, Sendai, Miyagi-ken, Japan; [3]Department of Geriatric Medicine, Graduate School of Medicine, The University of Tokyo, Hongo, Bunkyo-ku, Tokyo, Japan; and [4]Research Center for Genomic Medicine and Department of Molecular Biology, Saitama Medical School, Yamane, Hidaka-shi, Saitama, Japan
Received 1/6/05; revised 6/9/05; accepted 6/28/05.

Grant support: Ministry of Health, Labor, and Welfare Japan, the Ministry of Education, Culture, Sports, Science and Technology Japan, the Core Research for Evolutional Science and Technology, and the Princess Takamatsu Cancer Research Fund (02-23402).

The costs of publication of this article were defrayed in part by the payment of page charges. This article must therefore be hereby marked *advertisement* in accordance with 18 U.S.C. Section 1734 solely to indicate this fact.

Requests for reprints: Takashi Suzuki, Department of Pathology, Tohoku University School of Medicine, 2-1 Seiryo-machi, Aoba-ku, Sendai, 980-8575, Japan. Phone: 81-22-717-8050; Fax: 81-22-717-8051; E-mail: t-suzuki@patholo2.med.tohoku.ac.jp.

doi:10.1158/1078-0432.CCR-05-0040

Materials and Methods

Patients and tissues. Thirty specimens of invasive ductal carcinoma were obtained from patients who underwent mastectomy in 2001 in the Department of Surgery at Tohoku University Hospital, Sendai, Japan. Specimens for RNA isolation were snap-frozen and stored at −80°C, and those for immunohistochemistry were fixed with 10% formalin and embedded in paraffin wax. Informed consent was obtained from all patients before their surgery and examination of specimens used in this study.

One hundred fifty-one specimens of invasive ductal carcinoma of the breast were obtained from female patients who underwent mastectomy from 1982 to 1989 in the Department of Surgery, Tohoku University Hospital, Sendai, Japan. All specimens were fixed with 10% formalin and embedded in paraffin wax, and snap-frozen tissues were not available for examination in these cases. These patients did not receive any preoperative radiotherapy and chemotherapy as well as any postoperative hormone therapy. Information on patient age, menopausal status, stage, tumor size at operation, lymph node status, histologic grade, and relapse and survival times was retrieved from the review of patient charts. The mean follow-up period was 105 months (3-157 months).

Research protocols for this study were approved by the Ethics Committee at Tohoku University School of Medicine.

Immunohistochemistry. Anti-human Efp antibody was generated as previously described (3). Polyclonal antibody for 14-3-3σ (N-14) and monoclonal antibodies for ERα (1D5), progesterone receptor (MAB429), Ki-67 (MIB-1), and p53 (DO7) were purchased from Santa Cruz Biotechnology (Santa Cruz, CA), Immunotech (Marseille, France), Chemicon (Temecula, CA), DAKO (Tokyo, Japan), and Novocastra Laboratories (Newcastle, United Kingdom), respectively. A Histofine Kit (Nichirei, Tokyo, Japan), which employs the streptavidin-biotin amplification method, was used for immunohistochemistry, and the antigen-antibody complex was visualized with 3.3′-diaminobenzidine solution [1 mmol/L 3,3′-diaminobenzidine, 50 mmol/L Tris-HCl buffer (pH 7.6), and 0.006% H_2O_2]. For a negative control for Efp immunohistochemistry, an immunohistochemical preabsorption test was done.

Efp immunoreactivity was classified into three groups: ++, >50% positive carcinoma cells; +, 1% to 50% positive cells; and −, no immunoreactivity, according to a previous report (10). Immunoreactivity of ERα, progesterone receptor, and Ki-67 was scored in more than 1,000 carcinoma cells for each case, and the percentage of immunoreactivity [i.e., labeling index (LI)] was determined. Cases that were found to have ERα LI of more than 10% were considered ERα-positive breast carcinomas (11).

Laser capture microdissection/real-time PCR. Laser capture microdissection was conducted using the Laser Scissors CRI-337 (Cell Robotics, Inc., Albuquerque, NM). A detailed procedure has been described previously (12, 13). Briefly, ~1,000 carcinoma or intratumoral stromal cells were separately collected under the microscope from breast carcinoma frozen tissue sections embedded in Tissue-Tek O.T.C. The Light Cycler System (Roche Diagnostics GmbH, Mannheim, Germany) was used to semiquantify the level of Efp mRNA expression in this study. The primers used for real-time PCR were the following: Efp sense, 5′-CGTGGAGTGGTTCAACAC-3′, and Efp antisense, 5′-GAGCAGATGGAGAGTGTGG-3′; glyceraldehyde-3-phosphate dehydrogenase sense, 5′-TGAACGGGAAGCTCACTGG-3′, and glyceraldehyde-3-phosphate dehydrogenase antisense, 5′-TCCACCACCCTGTTGCTGTA-3′. To verify amplification of the correct sequences, PCR products were purified and subjected to direct sequencing. Efp mRNA levels were normalized to those of glyceraldehyde-3-phosphate dehydrogenase, and subsequently, the fold change of Efp mRNA level in each sample was evaluated using the mRNA level in MCF7 cells as a positive control. Negative control experiments lacked cDNA substrate to check for the possibility of exogenous contaminant DNA, and no amplified products were detected under these conditions.

Statistical analyses. Statistical analyses were done using one-way ANOVA and Bonferroni test or a cross-table using χ^2 test. Overall and disease-free survival curves were generated according to the Kaplan-Meier method, and statistical significance was calculated using log-rank test. Univariate and multivariate analyses were evaluated by a proportional hazard model (Cox) using PROC PHREG in our SAS software. Differences with $P < 0.05$ were considered significant.

Results

Expression of Efp in 30 breast cancer tissues: Immunohistochemistry. Efp immunoreactivity was detected in the cytoplasm of breast carcinoma cells, but not in intratumoral

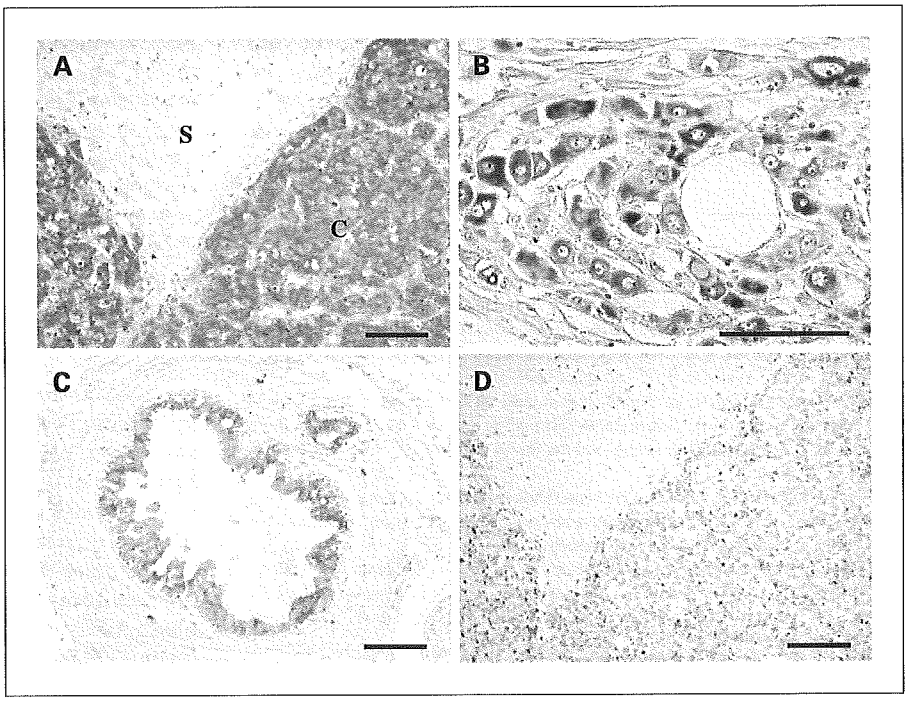

Fig. 1. Immunohistochemistry for Efp in breast carcinoma (invasive ductal carcinoma). *A* and *B*, Efp immunoreactivity was detected in the cytoplasm of the carcinoma cells (*C*), but not in intratumoral stromal cells (*S*). *C*, in morphologically normal mammary glands, Efp immunoreactivity was also detected in the epithelial cells. *D*, no significant immunoreactivity of Efp was detected in a section analyzed by immunohistochemical preabsorption test as a negative control. Same area as *A*. *Bar*, 100 μm.

stromal cells (Fig. 1A and B). The number of cases expressing immunoreactive Efp in each group of 30 breast carcinoma tissues is summarized as follows: ++, n = 9 (30.0%); +, n = 13 (43.3%); and −, 17 (56.7%). Efp immunoreactivity was also positive in epithelial cells of morphologically normal mammary glands (Fig. 1C). Immunohistochemical preabsorption test for Efp showed no specific immunoreactivity in a negative control (Fig. 1D).

Laser capture microdissection/real-time PCR. To examine the localization of Efp mRNA in breast carcinoma tissues, we did laser capture microdissection/real-time PCR analyses. Expression of Efp mRNA was detected in carcinoma cells, but not in intratumoral stromal cells (Fig. 2A). As shown in Fig. 2B, a significant association was detected between Efp immunoreactivity and Efp mRNA level (P = 0.0012, ++ versus − and ++ versus +, respectively) in 30 cases of breast cancer tissues examined.

Correlation between Efp immunoreactivity and clinicopathologic variables in 151 breast carcinomas. Results of associations between Efp immunoreactivity and clinicopathologic variables in 151 breast carcinomas were summarized in Table 1. The number of cases expressing immunoreactive Efp in each group is summarized as follows: ++, n = 46 (30.5%); +, n = 64 (42.4%); and −, n = 41 (27.2%). Efp immunoreactivity was significantly associated with lymph node status (P = 0.0027), ERα status (P = 0.0013), or ERα LI (P = 0.0023, ++ versus −; P = 0.0045, + versus −). On the other hand, negative correlation was detected between Efp immunoreactivity and histologic grade (P = 0.0064) or 14-3-3σ immunoreactivity (P < 0.0001). There was, however, no significant relationship between Efp immunoreactivity and other clinicopathologic variables, including patient age, menopausal status, stage, tumor size, progesterone receptor LI, Ki-67 LI, and 53 status, in this study. Similar tendencies described above were confirmed in increased rankings of positivity for Efp immunoreactivity into five groups (0%, 1-25%, 26-50%, 51-75%, and 76-100% positive cells; data not shown).

Correlation between Efp immunoreactivity and clinical outcome of the 151 breast cancer patients. Efp immunoreactivity was significantly associated with an increased risk of recurrence (P < 0.0001; Fig. 3A). A similar tendency was also detected when Efp immunoreactivity was further categorized into five groups (0%, 1-25%, 26-50%, 51-5%, and 76-100% positive cells; Fig. 3B). Following univariate analysis by Cox (Table 2), lymph node status (P < 0.0001), Efp immunoreactivity (P < 0.0001), tumor size (P = 0.0019), and 14-3-3σ immunoreactivity (P = 0.0314) were shown as significant prognostic variables for disease-free survival in 151 breast carcinoma patients examined. A multivariate analysis revealed that lymph node status (P < 0.0001), Efp immunoreactivity (P = 0.0011), and tumor size (P = 0.0349) were independent prognostic factors with relative risks over 1.0, whereas 14-3-3σ immunoreactivity was not significant (P = 0.0681; Table 2).

Overall survival curve was shown in Fig. 3C. A significant correlation was detected between Efp immunoreactivity and adverse clinical outcome of the patients (P < 0.0001), and a similar tendency was also detected when Efp immunoreactivity was categorized into five groups (Fig. 3D). Using a univariate analysis (Table 3), Efp immunoreactivity (P < 0.0001), lymph node status (P < 0.0001), tumor size (P = 0.0084), and p53 status (P = 0.0230) turned out to be

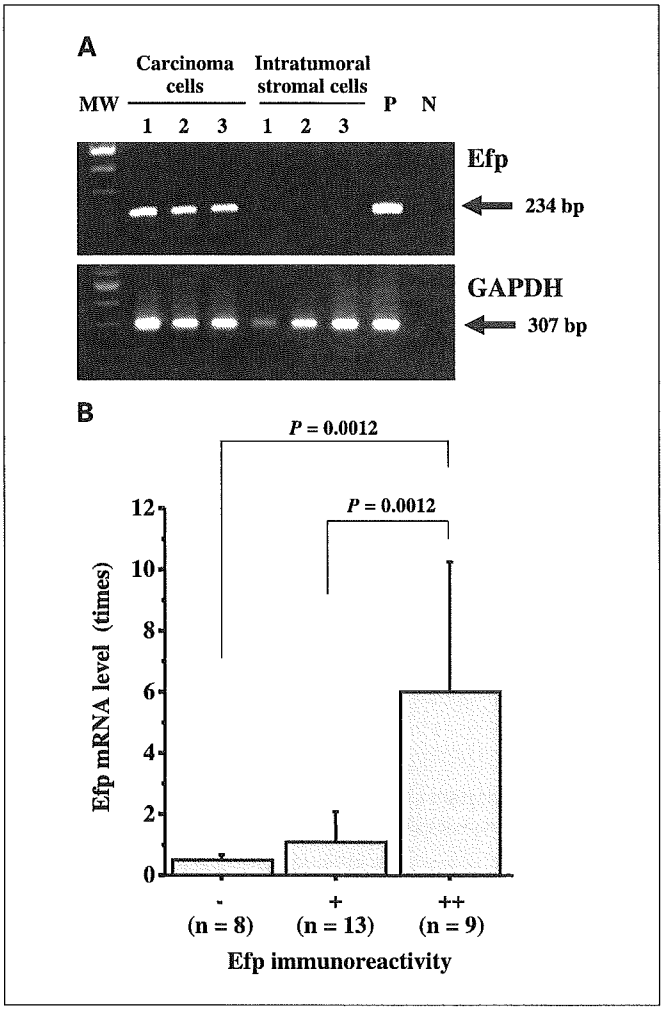

Fig. 2. Laser capture microdissection/real-time PCR analysis for Efp in breast carcinoma tissues. *A*, expression for Efp mRNA (234 bp) was detected only in the component of breast carcinoma cells, whereas that of glyceraldehyde-3-phosphate dehydrogenase (*GAPDH*) mRNA (307 bp) was detected in both components of carcinoma cells and intratumoral stromal cells. Three cases are represented in this agarose gel photo. PCR was done for 40 cycles. *P*, positive control (MCF7 cells); *N*, negative control (no cDNA substrate). *B*, association between Efp immunoreactivity and Efp mRNA level in the carcinoma cell component in 30 breast carcinoma tissues. A significant positive correlation was detected (P = 0.0012, ++ versus + and ++ versus −, respectively). Expression level of Efp mRNA in the carcinoma cell component of each case was represented as a ratio of that of glyceraldehyde-3-phosphate dehydrogenase, and was subsequently evaluated as the ratio (%) compared with that of MCF7 cells.

significant prognostic factors for overall survival in this study. However, multivariate analysis revealed that only Efp immunoreactivity (P = 0.0030) and lymph node status (P = 0.0065) were independent prognostic factors with a relative risk over 1.0; other factors were not significant in this study (Table 3).

The significant association between Efp immunoreactivity and clinical outcome of the patients was detected regardless of ERα status in this study (Fig. 4A-D).

Discussion

In this study, Efp immunoreactivity was significantly associated with Efp mRNA level, and was detected in carcinoma cells in 110 of 151 human breast carcinomas (72.8%).

Table 1. Association between Efp immunoreactivity and clinicopathologic variables in 151 human breast carcinomas

	Efp immunoreactivity			*P*
	++ (*n* = 46)	+ (*n* = 64)	– (*n* = 41)	
Age* (y)	52.8 ± 1.9	53.5 ± 1.6	52.4 ± 1.3	>0.05
Menopausal status				
Premenopausal	23 (15.2%)	33 (21.9%)	15 (9.9%)	
Postmenopausal	23 (15.2%)	31 (20.5%)	26 (17.2%)	>0.05
Stage				
I	11 (7.3%)	16 (10.6%)	11 (7.3%)	
II	26 (17.2%)	42 (27.8%)	26 (17.2%)	
III	9 (6.0%)	6 (31.6%)	4 (21.0%)	>0.05
Tumor size* (mm)	29.5 ± 2.5	24.1 ± 1.3	26.9 ± 3.0	>0.05
Lymph node status				
Positive	29 (19.2%)	20 (13.2%)	15 (9.9%)	
Negative	17 (11.3%)	44 (29.1%)	26 (17.2%)	0.0027
Histologic grade				
1	17 (11.3%)	17 (11.3%)	3 (2.0%)	
2	16 (10.6%)	22 (14.6%)	14 (9.3%)	
3	13 (8.6%)	25 (16.6%)	24 (15.9%)	0.0064
ERα status				
Positive	39 (25.8%)	49 (32.5%)	21 (13.9%)	
Negative	7 (4.6%)	15 (9.9%)	20 (13.2%)	0.0013
ERα LI*	48.9 ± 4.8	46.0 ± 4.2	27.0 ± 4.9	– vs ++; 0.0023 – vs +; 0.0045
Progesterone receptor LI*	46.8 ± 11.5	47.6 ± 4.3	34.6 ± 5.6	>0.05
14-3-3α immunoreactivity				
Positive	9 (6.0%)	20 (13.2%)	29 (19.2%)	
Negative	37 (24.5%)	44 (29.1%)	12 (7.9%)	<0.0001
Ki-67 LI*	23.9 ± 2.2	25.8 ± 2.2	27.2 ± 2.9	>0.05
P53 status				
Positive	13 (8.6%)	13 (8.6%)	17 (11.3%)	
Negative	33 (21.9%)	51 (33.8%)	24 (15.9%)	>0.05

*Data are presented as mean ± 95% confidence interval (95% CI). All other values represent the number of cases and percentage.

Previously, Ikeda et al. (5) reported Efp mRNA expression in 9 of 15 (60.0%) breast carcinoma tissues using RNase protection assay, and Thomson et al. (9) reported Efp immunoreactivity in breast carcinoma cells in 64 of 91 (70.3%) cases. The frequency and cellular localization of Efp in our present study were in good agreement with these reports (5, 9), and widespread distribution of Efp may suggest an important role of Efp in breast carcinomas. Efp immunoreactivity was also detected in normal glandular epithelia in our study. It is also consistent with previous studies (5, 9) and Thomson et al. (9) suggested the involvement of Efp in mammary gland differentiation.

Efp is known as a downstream product of ERα (3–7). *Efp* gene has an estrogen-responsive element at the 3′-untranslated region (3). The estrogen-responsive element of *Efp* responded to ERα in transfected estrogen receptors in 293T cells (5), and Efp mRNA was rapidly induced by estrogen treatment within 0.5 hour in MCF7 cells (5). In this study, Efp immunoreactivity was significantly associated with ERα status and ERα LI in 151 breast carcinoma tissues. Therefore, it is suggestive that Efp is mainly produced in carcinoma cells through ERα as a result of estrogenic action in breast carcinoma. On the other hand, we also found Efp immunoreactivity in 22 of 42 ERα-negative breast carcinomas. It may be partly explained that Efp expression was induced by a low or undetectable level of ERα in these cases. However, Ikeda et al. (14) analyzed human 5′-flanking region of human Efp gene, and reported the possible regulation of Efp promoter by multiple elements and/or interacting factors. Therefore, other factors rather than ERα may be also involved in the expression of Efp in some breast carcinomas.

In our study, Efp immunoreactivity was significantly associated with an increased risk of recurrence or worse prognosis ($P < 0.0001$, respectively). Both univariate and multivariate analyses have shown that Efp immunoreactivity was a potent prognostic factor for both recurrence and overall survival in breast carcinomas, and that the effect is similar to that of lymph node status, a well-established diagnostic modality (15). Efp knockout mice showed a smaller increase in uterine weight and a lower cell cycle progression from G_0/G_1 to S phase compared with the wild-type (7), suggesting a pivotal role of Efp in ERα-induced cell growth in the uterus. In addition, Urano et al. (8) showed that overexpression of Efp caused tumor cell growth in MCF7 breast cancer cells. Therefore, taken together with these previous reports and our present results, it is suggested that Efp

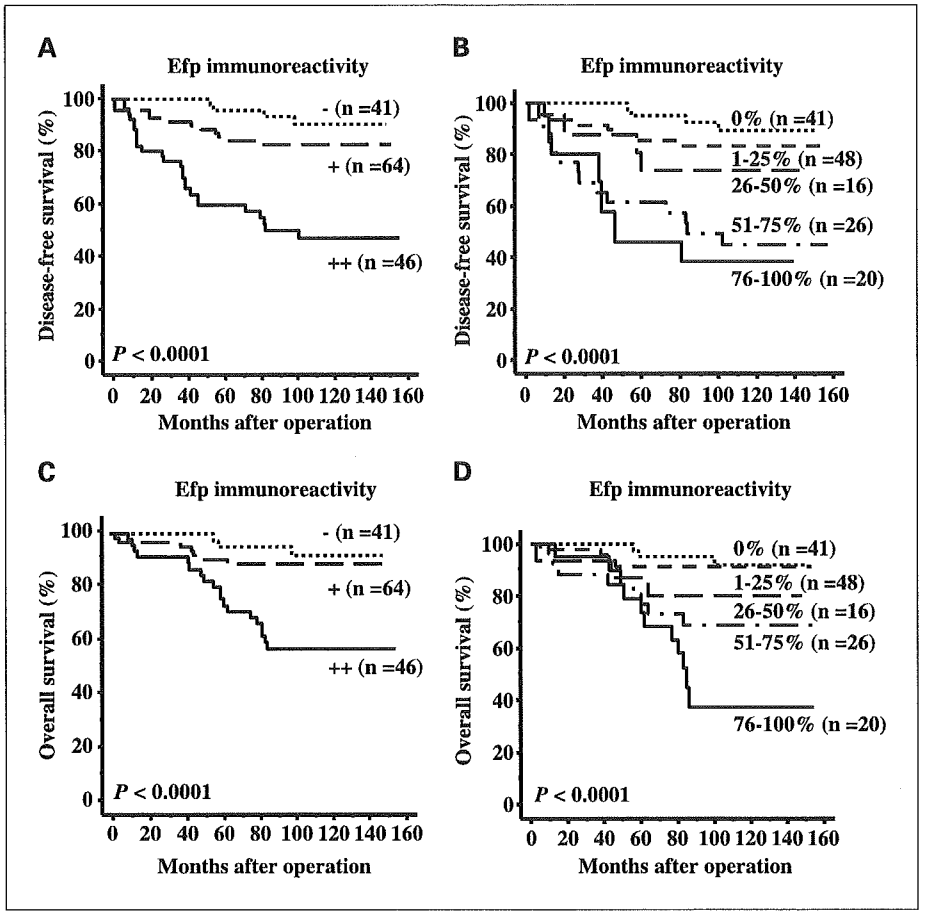

Fig. 3. Disease-free (*A* and *B*) and overall (*C* and *D*) survival of 151 patients with breast carcinoma according to Efp immunoreactivity (Kaplan-Meier method). *A*, Efp immunoreactivity was significantly ($P < 0.0001$, log-rank test) associated with an increased risk of recurrence. *B*, association between Efp immunoreactivity and increased risk of recurrence was also detected in increased rankings of positivity for Efp immunoreactivity into five groups (0%, 1-25%, 26-50%, 51-75%, and 76-100% positive cells). *C* and *D*, Efp immunoreactivity was significantly ($P < 0.0001$, log-rank test) associated with worse overall survival when Efp immunoreactivity was classified into three (*C*) or five (*D*) groups.

plays an important role in the proliferation of breast carcinoma cells. It is well known that biologically active estrogen, estradiol, is locally produced in breast carcinoma tissues from circulating inactive steroids, and acts on these cells via ERα (16). Therefore, residual cancer cells following surgical treatment in Efp-positive breast carcinomas may grow rapidly in the presence of local estrogens, thereby resulting in an increased recurrence and poor prognosis in these patients.

14-3-3σ induces G_2 arrest and inhibits the progression of cell cycle (17) by sequestering the mitotic initiation complex Cdc2-cyclin B1 in the cytoplasm, blocking nuclear entry (18). Expression of 14-3-3σ was examined by several groups in breast carcinoma tissues. However, results of these studies seem to be inconsistent. Ferguson et al. (19) reported that 14-3-3σ mRNA was detected only in 3 of 48 (6.3%) breast carcinoma tissues by Northern blot analysis. Ferguson et al. (19) and Umbricht et al. (20) showed hypermethylation of CpG islands in the 14-3-3σ gene in more than 90% of breast carcinomas, and postulated that loss of 14-3-3σ expression was an early event in neoplastic transformation of the breast. Simooka et al.

Table 2. Univariate and multivariate analyses of disease-free survival in 151 breast cancer patients examined

Variable	Univariate	Multivariate	
	P	*P*	Relative risk (95% CI)
Lymph node status (positive/negative)	<0.0001*	<0.0001	6.053 (2.549-14.379)
Efp immunoreactivity (++/+, −)	<0.0001*	0.0011	3.090 (1.572-6.073)
Tumor size (≥20 mm/<20 mm)	0.0019*	0.0349	3.157 (1.085-9.184)
14-3-3α immunoreactivity (negative/positive)	0.0314*	0.0681	
Ki-67 LI (≤10/<10)	0.1149		
ERα status (positive/negative)	0.1392		
Histologic grade (3/1, 2)	0.2362		
p53 status (positive/negative)	0.4094		

*Data were considered significant in the univariate analyses and were examined in the multivariate analyses.

Table 3. Univariate and multivariate analyses of overall survival in 151 breast cancer patients examined

Variable	Univariate	Multivariate	
	P	*P*	Relative risk (95% CI)
Efp immunoreactivity (++/+, −)	<0.0001*	0.0030	5.343 (1.725-16.175)
Lymph node status (positive/negative)	<0.0001*	0.0065	7.783 (1.773-34.166)
Tumor size (≥20 mm/<20 mm)	0.0084*	0.1514	
p53 status (positive/negative)	0.0230*	0.0832	
ERα status (positive/negative)	0.2890		
Ki-67 LI (≥10/<10)	0.3562		
Histologic grade (3/1, 2)	0.3827		
14-3-3α immunoreactivity (negative/positive)	0.6286		

*Data were considered significant in the univariate analysis and were examined in the multivariate analyses.

(21) detected 14-3-3σ immunoreactivity in 23% of invasive ductal carcinomas and reported that loss of 14-3-3σ expression was relatively low compared with the methylation status of 14-3-3σ gene in breast carcinoma previously reported. On the other hand, Urano et al. (8) showed that 14-3-3σ is a primary target for proteolysis by Efp, and 14-3-3σ protein was regulated by Efp-mediated posttranslational modification. However, Moreira et al. (22) recently reported that expression level of 14-3-3σ was similar in nonmalignant breast epithelial tissue and matched malignant tissue with only sporadic loss of expression observed in 3 of the 68 (4.4%) tumors examined. The lack of expression of 14-3-3σ in the three breast carcinomas was not associated with increased expression of Efp, and they suggested that loss of expression of 14-3-3σ protein was a sporadic event in the breast carcinoma (22). In our present study, immunoreactivity of 14-3-3σ was detected in 58 of 151 (38.4%) breast carcinomas, and was inversely associated with Efp immunoreactivity. These results seem to support the down-regulation of

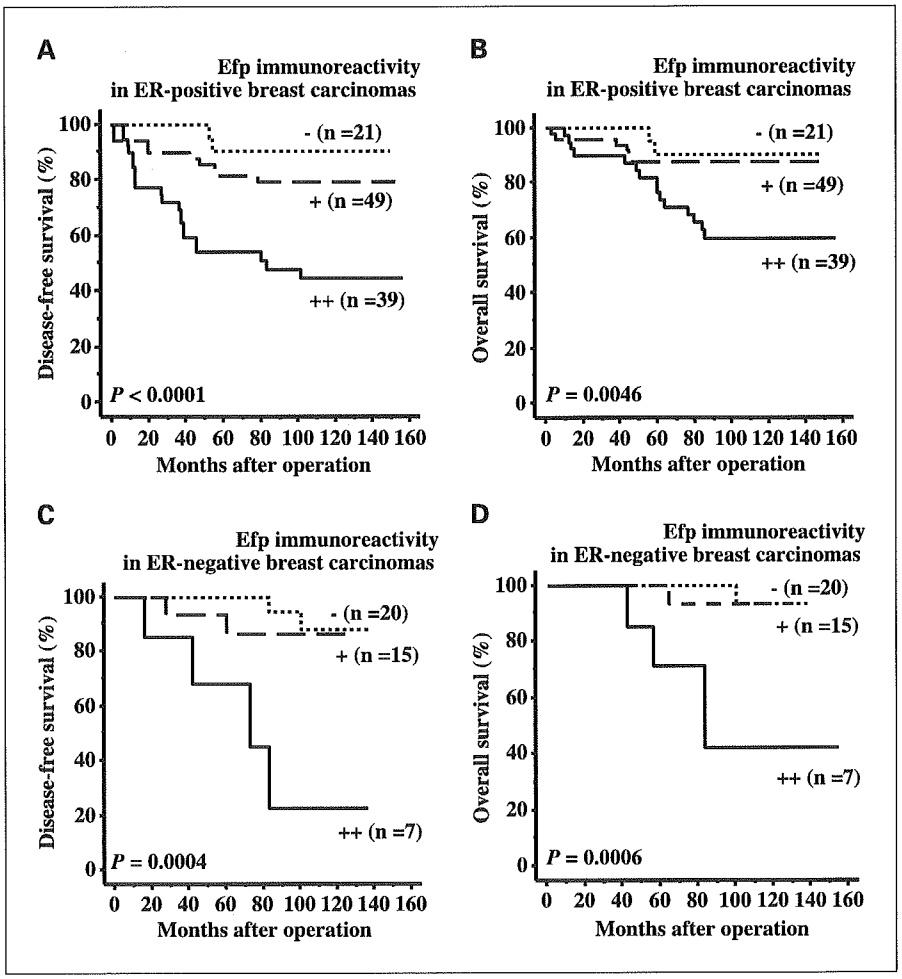

Fig. 4. Association between Efp immunoreactivity and disease-free (*A* and *C*) or overall (*B* and *D*) survival of 151 patients according to ERα status (Kaplan-Meier method). Efp immunoreactivity was significantly associated with poor clinical outcome of 151 breast cancer patients regardless of ERα status. Statistical association was evaluated by log-rank test.

14-3-3σ by methylation of the gene and/or proteolysis by Efp in breast carcinoma tissues; however, these are not necessarily consistent with the findings by Moreira et al. (22). Further examinations, including validation of the immunohistochemical results by another laboratories, are required to clarify the expression of 14-3-3σ in breast carcinoma tissues.

In summary, Efp immunoreactivity was detected in carcinoma cells in 72.8% of breast cancer tissues, and it was associated with the mRNA level. Efp immunoreactivity was significantly associated with lymph node status or ERα status, and was inversely correlated with histologic grade or 14-3-3σ immunoreactivity. Moreover, Efp immunoreactivity was significantly associated with poor clinical outcome of the patients. These present results suggest that Efp is mainly involved in the estrogen-dependent growth of breast carcinomas, and Efp immunoreactivity is a potent prognostic factor in breast carcinoma patients.

Acknowledgments

We appreciate the skillful technical assistance of Dr. Yasuhiro Miki (Department of Pathology, Tohoku University School of Medicine, Sendai, Japan) and Toshiki Hishinuma (Saitama Medical School, Hidaka, Japan). We thank Dr. Bruce Blumberg (Department of Developmental and Cell Biology, University of California, Irvine, CA) for critical reading and comments on the manuscript.

References

1. Ali S, Coombes RC. Endocrine-responsive breast cancer and strategies for combating resistance. Nat Rev Cancer 2002;2:101–12.
2. Jordan VC. Fourteenth Gaddum Memorial Lecture. A current view of tamoxifen for the treatment and prevention of breast cancer. Br J Pharmacol 1993;110:507–17.
3. Inoue S, Orimo A, Hosoi T, et al. Genomic binding-site cloning reveals an estrogen-responsive gene that encodes a RING finger protein. Proc Natl Acad Sci U S A 1993;90:11117–21.
4. Orimo A, Inoue S, Ikeda K, Noji S, Muramatsu M. Molecular cloning, structure, and expression of mouse estrogen-responsive finger protein Efp. Co-localization with estrogen receptor mRNA in target organs. J Biol Chem 1995;270:24406–13.
5. Ikeda K, Orimo A, Higashi Y, Muramatsu M, Inoue S. Efp as a primary estrogen-responsive gene in human breast cancer. FEBS Lett 2000;472:9–13.
6. Muramatsu M, Inoue S. Estrogen receptors: how do they control reproductive and nonreproductive functions? Biochem Biophys Res Commun 2000;270:1–10.
7. Orimo A, Inoue S, Minowa O, et al. Underdeveloped uterus and reduced estrogen responsiveness in mice with disruption of the estrogen-responsive finger protein gene, which is a direct target of estrogen receptor α. Proc Natl Acad Sci U S A 1999;96:12027–32.
8. Urano T, Saito T, Tsukui T, et al. Efp targets 14-3-3σ for proteolysis and promotes breast tumour growth. Nature 2002;417:871–5.
9. Thomson SD, Ali S, Pickles L, et al. Analysis of estrogen-responsive finger protein expression in benign and malignant human breast. Int J Cancer 2001;91:152–8.
10. Suzuki T, Nakata T, Miki Y, et al. Estrogen sulfotransferase and steroid sulfatase in human breast carcinoma. Cancer Res 2003;63:2762–70.
11. Allred DC, Harvey JM, Berardo M, Clark GM. Prognostic and predictive factors in breast cancer by immunohistochemical analysis. Mod Pathol 1998;11:155–68.
12. Emmert-Buck MR, Bonner RF, Smith PD, et al. Laser capture microdissection. Science 1996;274:998–1001.
13. Niino YS, Irie T, Takaishi M, et al. PKCθ II, a new isoform of protein kinase C specifically expressed in the seminiferous tubules of mouse testis. J Biol Chem 2001;276:36711–7.
14. Ikeda K, Inoue S, Orimo A, et al. Multiple regulatory elements and binding proteins of the 5′-flanking region of the human estrogen-responsive finger protein (efp) gene. Biochem Biophys Res Commun 1997;236:765–71.
15. Dowlatshahi K, Fan M, Snider HC, Habib FA. Lymph node micrometastases from breast carcinoma: reviewing the dilemma. Cancer 1997;80:1188–97.
16. Suzuki T, Moriya T, Ishida T, Ohuchi N, Sasano H. Intracrine mechanism of estrogen synthesis in breast cancer. Biomed Pharmacother 2003;57:460–2.
17. Hermeking H, Lengauer C, Polyak K, et al. 14-3-3σ is a p53-regulated inhibitor of G_2/M progression. Mol Cell 1997;1:3–11.
18. Chan TA, Hermeking H, Lengauer C, Kinzler KW, Vogelstein B. 14-3-3σ is required to prevent mitotic catastrophe after DNA damage. Nature 1999;401:616–20.
19. Ferguson AT, Evron E, Umbricht CB, et al. High frequency of hypermethylation at the 14-3-3σ locus leads to gene silencing in breast cancer. Proc Natl Acad Sci U S A 2000;97:6049–54.
20. Umbricht CB, Evron E, Gabrielson E, Ferguson A, Marks J, Sukumar S. Hypermethylation of 14-3-3σ (stratifin) is an early event in breast cancer. Oncogene 2001;20:3348–53.
21. Simooka H, Oyama T, Sano T, Horiguchi J, Nakajima T. Immunohistochemical analysis of 14-3-3σ and related proteins in hyperplastic and neoplastic breast lesions, with particular reference to early carcinogenesis. Pathol Int 2004;54:595–602.
22. Moreira JM, Ohlsson G, Rank FE, Celis JE. Down-regulation of the tumor suppressor protein 14-3-3σ is a sporadic event in cancer of the breast. Mol Cell Proteomics 2005;4:555–69.

J Hum Genet (2005) 50:235–240
DOI 10.1007/s10038-005-0244-x

ORIGINAL ARTICLE

**Yoshihiro Sudo · Yoichi Ezura · Mitsuko Kajita
Hideyo Yoshida · Takao Suzuki · Takayuki Hosoi
Satoshi Inoue · Masataka Shiraki · Hiromoto Ito
Mitsuru Emi**

Association of single nucleotide polymorphisms in the promoter region of the pro-opiomelanocortin gene (*POMC*) with low bone mineral density in adult women

Received: 10 December 2004 / Accepted: 23 February 2005 / Published online: 29 April 2005

Abstract Among multiple factors influencing osteoporosis, genetic variations involved in bone-mineral metabolism can affect risks predisposing to the disease onset. Here, we studied single-nucleotide polymorphisms (SNPs) in the pro-opiomelanocortin (*POMC*) gene for possible association with bone mineral density (BMD) among 384 adult Japanese women and observed significant correlation between adjusted BMD and three SNPs in the promoter region ($r > 0.14$, $p < 0.01$). The most significant correlation was observed for −2353G/A ($r = -0.16$, $p = 0.002$); homozygous carriers of the major (G) allele had the highest BMD (0.405 ± 0.054 g/cm^2) while heterozygous carriers were intermediate (0.390 ± 0.053 g/cm^2) and homozygous A-allele carriers had the lowest BMDs (0.369 ± 0.048 g/cm^2). Although no association was detected between these SNPs and body weight or body mass index (BMI), significant association was detected between the −2313A/C genotype and plasma total cholesterol level ($r = -0.12$, $p = 0.019$). We propose that *POMC* is among the likely susceptibility genes for osteoporosis and may also be involved in dyslipidemia.

Keywords Single nucleotide polymorphism · Pro-opiomelanocortin (POMC) · Bone mineral density · Association study · Osteoporosis

Y. Sudo · Y. Ezura · M. Kajita · M. Emi
Department of Molecular Biology,
Institute of Gerontology,
Nippon Medical School Kawasaki,
Kanagawa, Japan

Y. Sudo · H. Ito
Department of Orthopaedics,
Nippon Medical School,
Tokyo, Japan

H. Yoshida · T. Suzuki
Epidemiology and Health Promotion Research Group,
Tokyo Metropolitan Institute of Gerontology,
Tokyo, Japan

T. Hosoi
Department of Endocrinology,
Tokyo Metropolitan Geriatric Hospital,
Tokyo, Japan

S. Inoue
Department of Geriatric Medicine,
Faculty of Medicine,
University of Tokyo,
Tokyo, Japan

M. Shiraki
Research Institute and Practice for Involutional Diseases,
Nagano, Japan

Present address: Y. Ezura (✉)
Department of Molecular Pharmacology
Institute of Medical Research,
Tokyo Medical and Dental University,
2-3-10 Kanda-Surugadai,
Chiyoda-ku, Tokyo 101-0062, Japan
E-mail: ezura.mph@mri.tmd.ac.jp
Tel.: +81-3-52808067
Fax: +81-3-52808067

Introduction

Osteoporosis, one of the most prevalent disease conditions in older age groups, is pathologically defined by low bone mineral density (BMD) and deterioration of bone structure (Riggs and Melton 1986; Kanis et al. 1994). Like many other common diseases, multiple factors, including genetic variations, determine predisposition for onset or progression of osteoporosis, as has been indicated by genetic–epidemiological studies (Peacock et al. 2002; Albagha and Ralston 2003). Numerous studies on genetic risks for osteoporosis have been investigated to date, mainly by association studies and linkage analysis for quantitative trait BMD (Liu et al. 2003).

Among those studies, a quantitative trait locus (QTL) for spinal BMD has been identified in the chromosomal region 2p23–24 in large Caucasian pedigrees (Devote